4.2.3 1/5 Scale Test

1) Objectives

(1) Confirm the operational characteristics of the flow damper

Observation of the flow in the flow damper during large and small flow, large/small flow switching, and confirmation of the expected behavior of the flow

(2) Confirm the performance characteristics during large and small flow by measurement

The cavitation factor and flow rate coefficient during both flow conditions were measured, and confirm the flow characteristics are similar to the expected ACC performance. The flow characteristics obtained by the test were compared with the results of the full height 1/2 scale test later in this report and are used to confirm the validity of applying the scaling basis for these experiments.

2) Test apparatus

The outline drawings of the test apparatus is shown in Fig. 4.2.3-1. The test facility consists of a test tank, flow damper, standpipe, injection piping and exhaust tank. The flow damper made of transparent acrylate was installed outside of the test tank, thereby allowing fluid characteristics in the flow damper to be observed. A ball valve (nominal diameter is [ ] [ ] is provided on the injection line as the isolation valve and a gate valve (nominal diameter is [ ] is also provided on the injection line to control the flow resistance.

Fig. 4.2.3-1 Outline Drawing of the Visualization Test Apparatus

The specifications of the test facility are as follows:

(1) Test tank

Design Pressure	:	[ ]
Diameter	:	
Height	:	
Volume	:	

(2) Flow damper and standpipe (1/5 scale of the Actual size)

Diameter of vortex chamber	:	[ ]
Height of vortex chamber	:	
Shape of standpipe	:	

(3) Injection piping

Inner diameter (Simulating the pressure drop)	:	[ ]

(4) Exhaust tank

Design Pressure	:	[ ]
Diameter	:	
Height	:	
Volume	:	

3) Testing method

(a) Visualization test method

(1) Visualization tests were conducted for three cases: (i) examining flow characteristics during large flow injection and flow switching, setting the initial pressure at [ ], which is the maximum design pressure of the test tank; (ii) examining flow characteristics during small flow injection, setting the initial pressure at [ ] for a long small flow injection time, and (iii) examining flow characteristics during flow switching, setting the initial pressure at [ ], which has the same Froude number as that of the actual plant condition.

(2) The flow characteristics in the flow damper were recorded and observed using a video camera, shown in Fig.4.2.3-1.

(3) The characteristics of the flow in the vortex chamber were observed using blue ink as a flow tracer.

(b) Low pressure injection testing method

(1) The test tank pressure, test tank water level, damper outlet pressure, and exhaust tank pressure were measured and input into a PC to calculate the flow rate coefficient and the cavitation factor.

(2) Flow rate coefficient and cavitation factor were obtained by the following equations:

Flow rate coefficient C_V

$$C_V = \frac{1}{\sqrt{K_D}} \tag{4-7}$$

$$K_D = \frac{(P_A + \rho g H) - (P_D + \rho {V_D}^2 / 2 + \rho g H')}{\rho V_D^2 / 2} \tag{4-8}$$

Cavitation factor σ_v

$$\sigma_v = \frac{P_D + P_{at} - P_v}{(P_A + \rho g H) - (P_D + \rho V_D^2 / 2 + \rho g H')} \tag{4-9}$$

Where

K_D	:	Resistance coefficient of flow damper
P_A	:	Test tank pressure [gage]
ρ	:	Density of water
g	:	Acceleration of gravity
H	:	Distance between test tank water level and vortex chamber
H'	:	Distance between outlet pipe and vortex chamber
P_{at}	:	Atmospheric pressure
P_v	:	Vapor pressure of water
P_D	:	Static pressure of flow damper outlet piping [gage] Note
V_D	:	Velocity in the flow damper outlet piping Note

Note: These parameters were the values converted to the scale of the actual ACC

(3) Data Processing

Data smoothing techniques were utilized to eliminate noises from data of the ACC water level, the ACC pressure and the flow damper outlet pressure data processing and is discussed.

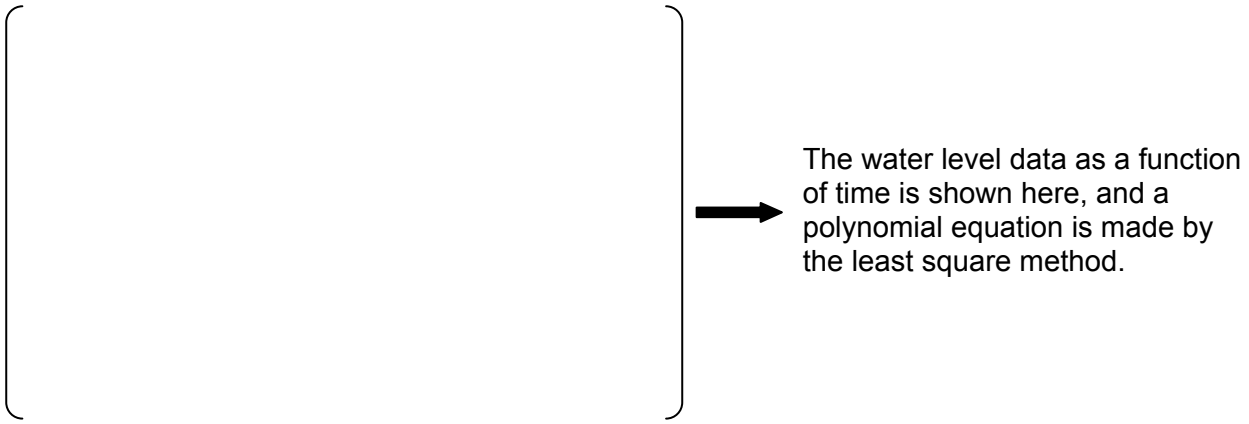

(a) Data of the ACC water level

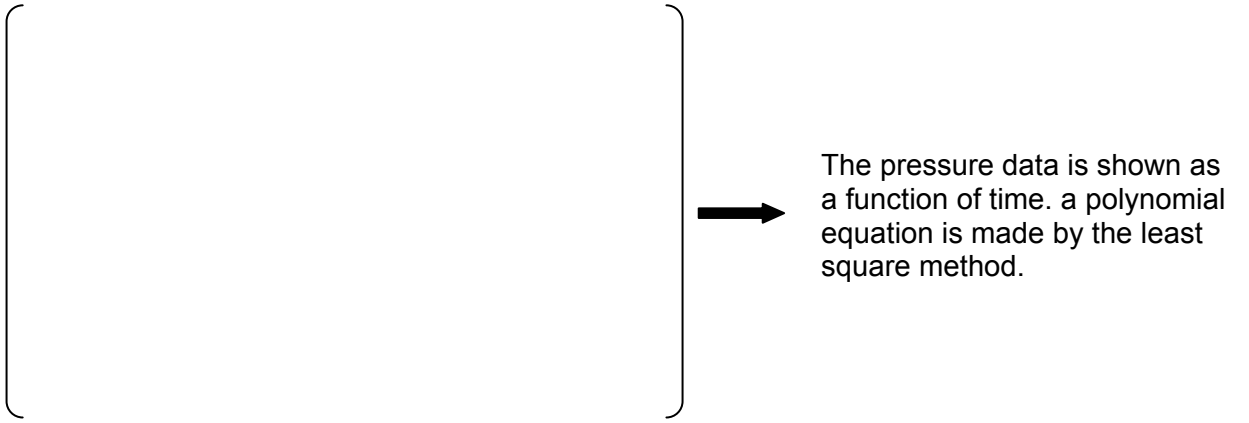

(b) Data of the ACC pressure

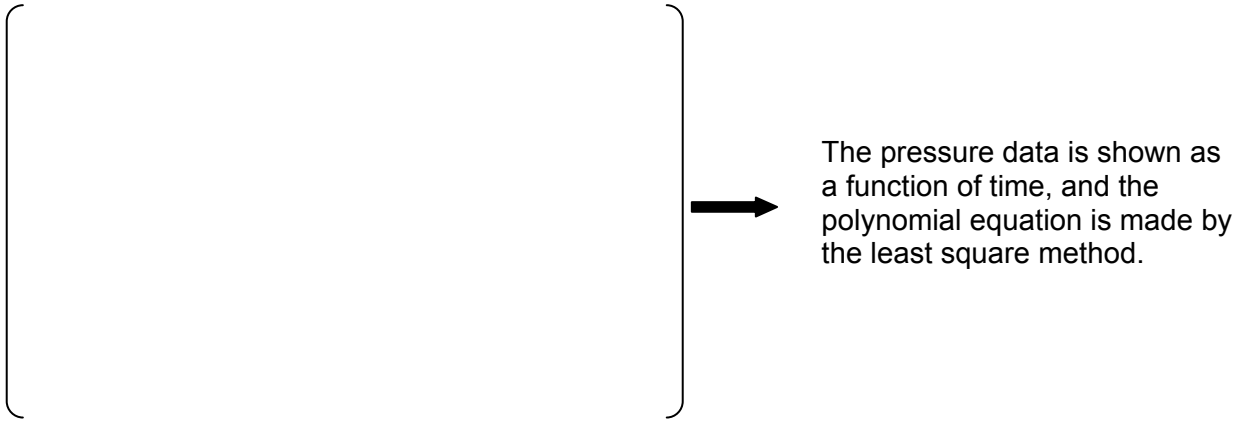

(c) Data of the Flow Damper outlet pressure

4) Test Conditions

Visualization Test Conditions

Visualization test conditions are shown in Table 4.2.3-1.

Low Pressure Injection Test Conditions

Low pressure test conditions are shown in Table 4.2.3-2.
The purpose of this test was to confirm the flow characteristics of the flow damper during large flow with wide variations of cavitation factors. The initial pressure conditions for the test tank and the exhaust tank were set at values that facilitated the testing.

Table 4.2.3-1 Visualization Test Conditions

Table 4.2.3-2 Low Pressure Injection Test Conditions

5) Parameters and Measuring Equipment

Pressure, water level and temperature were measured to calculate cavitation factors and flow rate coefficients. The differential pressure transducer measuring water level in tank and the attachments of pressure transducer are shown in Fig. 4.2.3-1.

6) Test Results and Consideration

a) The Visualization Test Results

The visualization test results are listed in Table 4.2.3-3 and the flow in the vortex chamber during large, large/small switching and small flow are shown in Photos. 4.2.3-1 to 4.2.3-3. The white lines are added in the photos to show the tracer trajectories clearly.

(1) The characteristic of the large flow is shown in Photo. 4.2.3-1. Since the flow tracer traveled from the point of the flow from the standpipe directly to the flow damper exit following collision with the water from the small flow inlet, it was confirmed that a vortex was not formed in the vortex chamber during large flow injection.

(2) The characteristic of the large/small flow switching is shown in Photo. 4.2.3-2. It shows transient status forming vortex under flow rate switching. It was also confirmed that gas entrainment from the standpipe did not occur and the flow rate switched smoothly in a short time.

(3) The characteristic of small flow is shown in Photo. 4.2.3-3. It was confirmed that the flow tracer swirled to the outlet, and a stable vortex was formed in the vortex chamber.

Table 4.2.3-3 Visualization Test Results

Test Number (T. No.)	Initial pressure [Test Tank]	Large flow	Flow rate switching	Small flow
1/5- 1-1		A vortex was not formed in the vortex chamber during large flow.	The flow rate switched smoothly in a short time.	-
1/5- 1-2		-	-	A stable vortex was formed in the vortex chamber.
1/5-1-3		-	The flow rate switched smoothly in a short time.	-

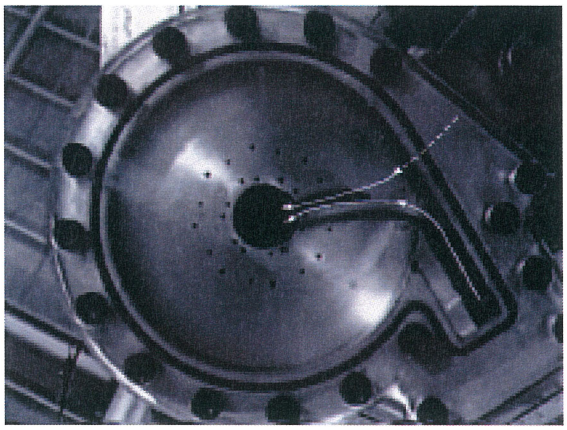

Photo. 4.2.3-1 Large Flow

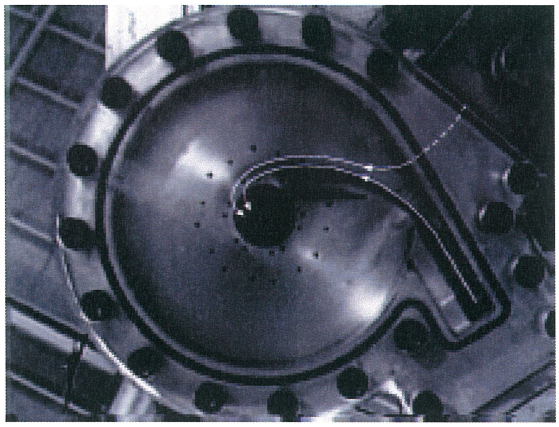

Photo. 4.2.3-2 Switching Flow Rate

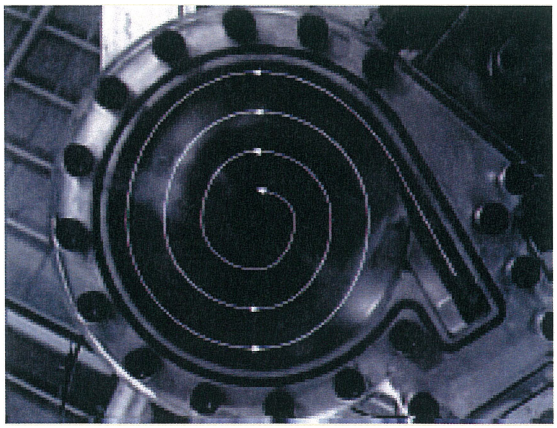

Photo. 4.2.3-3 Small Flow

b) Low Pressure Injection Test Results

This test was conducted at low pressure using a 1/5 scale model and the following results were obtained.

(1) The test tank pressure and water level and the outlet pressure of the flow damper as a function of time are shown in Figs. 4.2.3-2(1/2),(2/2) to 4.2.3-4(1/2),(2/2). It was confirmed that the test tank water level decreased steeply during large flow and decreased gently after the flow rate switching to small flow.

(2) The relation between the flow rate coefficient and cavitation factor in the flow damper is shown in Figs. 4.2.3-2 (2/2) to 4.2.3-4(2/2)[Note]. The behavior of large flow injection shows that the flow rate coefficient increased when the cavitation factor increased and became almost constant when the cavitation factor was greater than[ ].

Note: The data during almost steady condition were plotted.

(3) The relation between the flow rate coefficient and cavitation factor in the flow damper during small flow is also shown. It is shown that the flow rate coefficient during small flow was constant and independent of the cavitation factor.

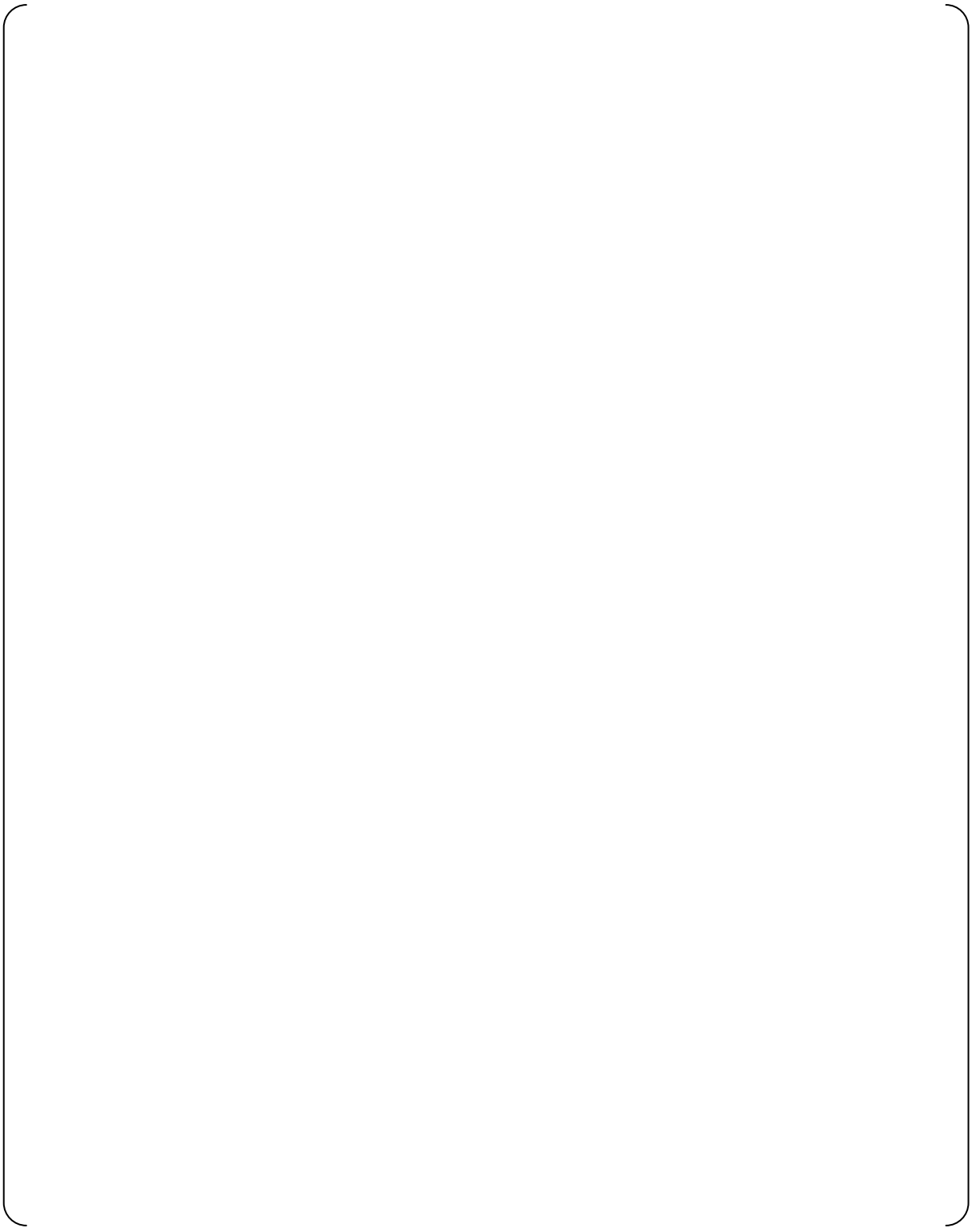

Fig. 4.2.3-2 (1/2) Low Pressure Injection Test Results (T. No. 1/5-2-1) 1/2

Fig. 4.2.3-2 (2/2) Low Pressure Injection Test Results (T. No. 1/5-2-1) 2/2

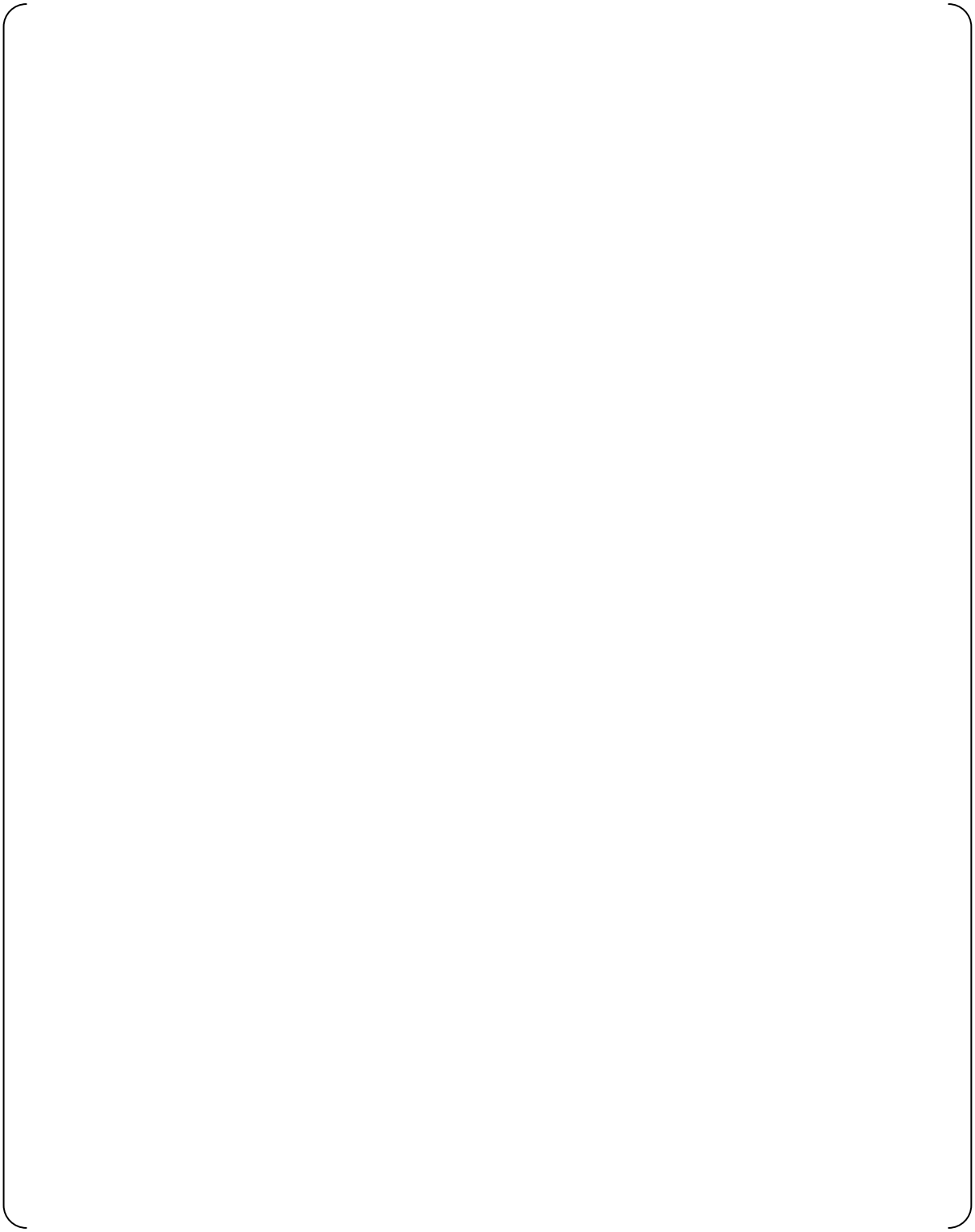

Fig. 4.2.3-3(1/2) Low Pressure Injection Test Results (T. No. 1/5-2-2) 1/2

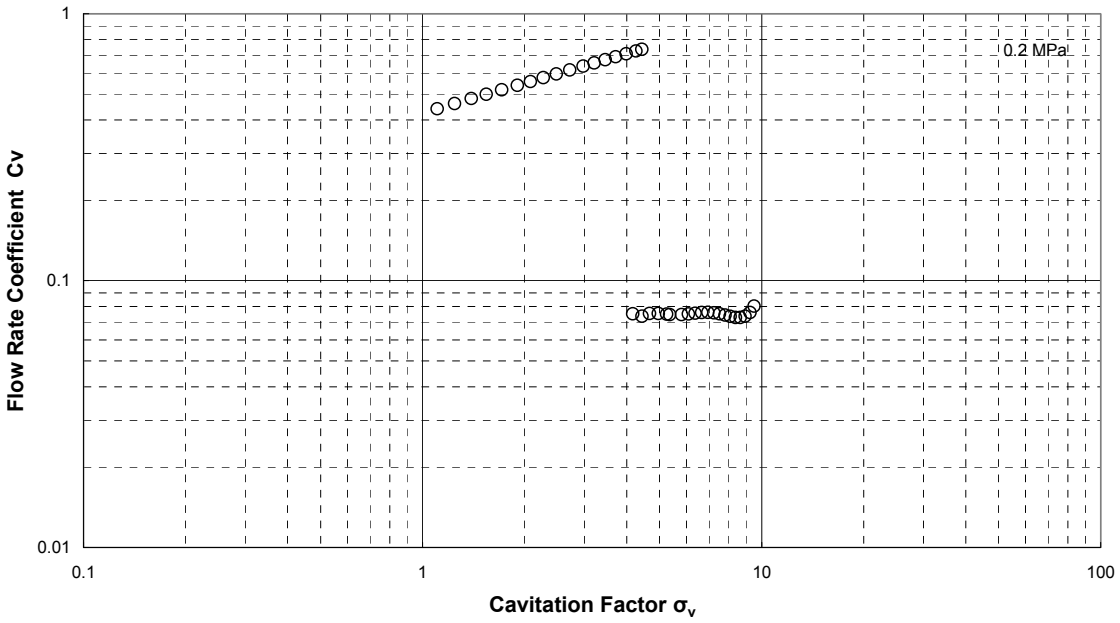

Fig. 4.2.3-3 (2/2) Low Pressure Injection Test Results (T. No. 1/5-2-2) 2/2

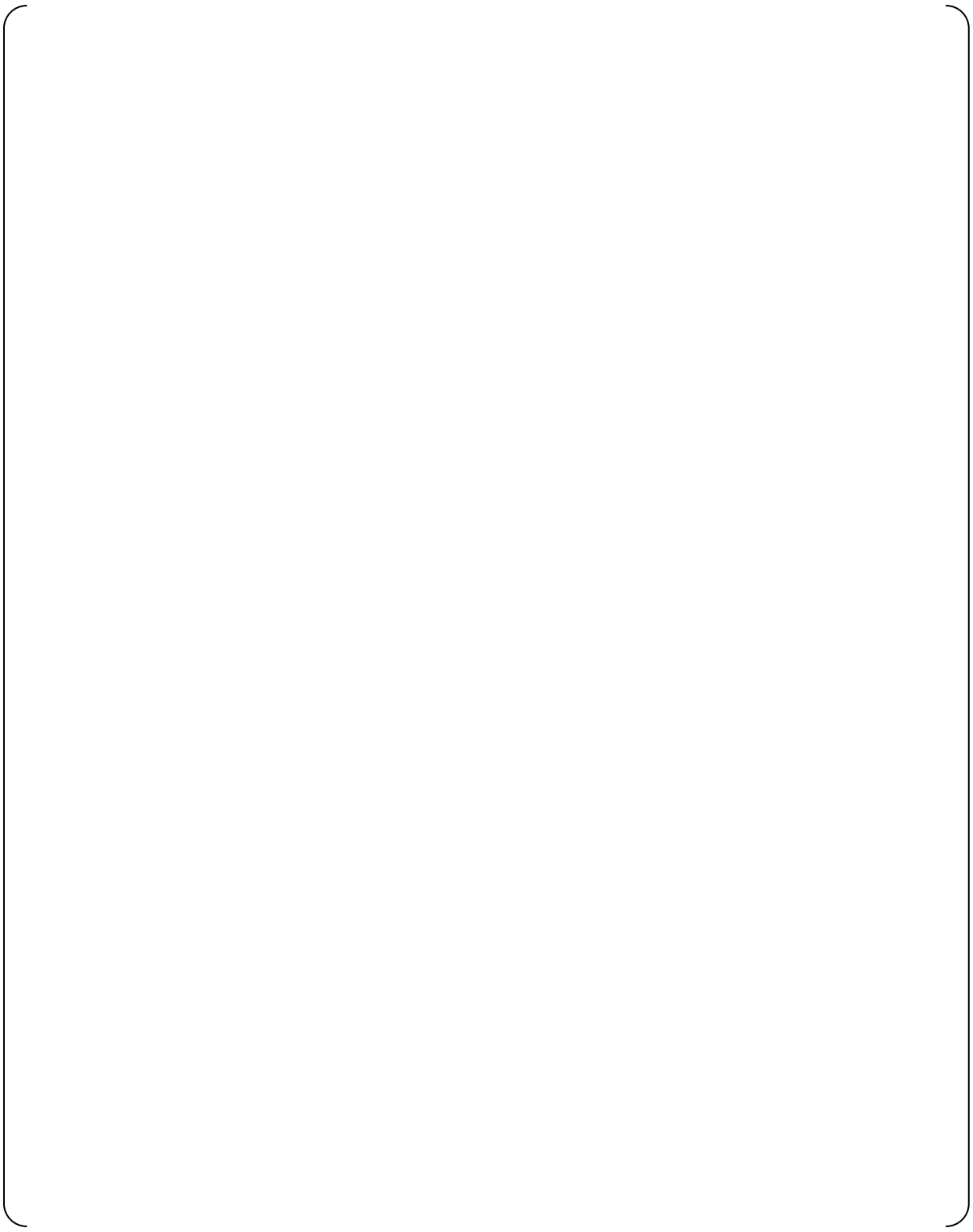

Fig. 4.2.3-4 (1/2) Low Pressure Injection Test Results (T. No. 1/5-2-3) 1/2

Fig. 4.2.3-4(2/2) Low Pressure Injection Test Results (T. No. 1/5-2-3) 2/2

4.2.4 Full Height 1/2 Scale Test

1) Objectives

(1) Obtainment of the flow characteristic data and confirmation of no gas entrainment
The test was conducted to obtain the flow characteristic data in the flow damper and to confirm that gas entrainment through the standpipe is prevented during flow switching and small flow injection.

(2) Confirmation that the flow characteristics can be characterized by dimensionless numbers (cavitation factor and flow rate coefficient)
Since a throat was added at the vortex chamber outlet to form strong vortex, it was assumed that cavitation might occur at the throat. The cavitation phenomenon is characterized by the cavitation factor which can be evaluated. It was confirmed by test that the flow rate coefficient is characterized by cavitation factor.

(3) Confirmation of the flow switching water level
The flow rate, as expected, switched from large flow to small flow when the water level decreased to the lower end of the standpipe cap. However, it is assumed that the water switching level may vary in the actual accumulator. Therefore, the actual switching water level was confirmed.

(4) Confirmation of the effect of dissolved nitrogen gas
Since the accumulator tank is pressurized by nitrogen gas, it is assumed that nitrogen gas dissolves into the water. If the water contains dissolved nitrogen gas, the dissolved gas may come out of solution during injection and affect the flow characteristics of the flow damper. Therefore, the test was conducted to evaluate the effect of dissolved gas on the injection flow.

2) Test Facility

The schematic and outline drawing of the test facility and the general flow path are shown in Fig. 4.2.4-1 and Fig. 4.2.4-2. The test facility consists of a test tank, flow damper, injection piping and exhaust tank. The flow damper is installed in the test tank. The height of the test tank and the standpipe is the full scale height and the inner diameter of the test tank is 1/2 scale (Fig. 4.2.4-3 and Fig. 4.2.4-4). Therefore, the water volume is 1/4 scale and the flow rate is also 1/4 scale. The test was conducted simulating the actual time. In addition, the water level transient during flow switching in the standpipe can be observed to represent the level transient in the actual standpipe. A ball valve is provided on the injection line as the isolation valve and a gate valve is provided on the injection line to control flow resistance. A pressure control valve is provided on the upper side of the test tank to control the tank pressure during the test.

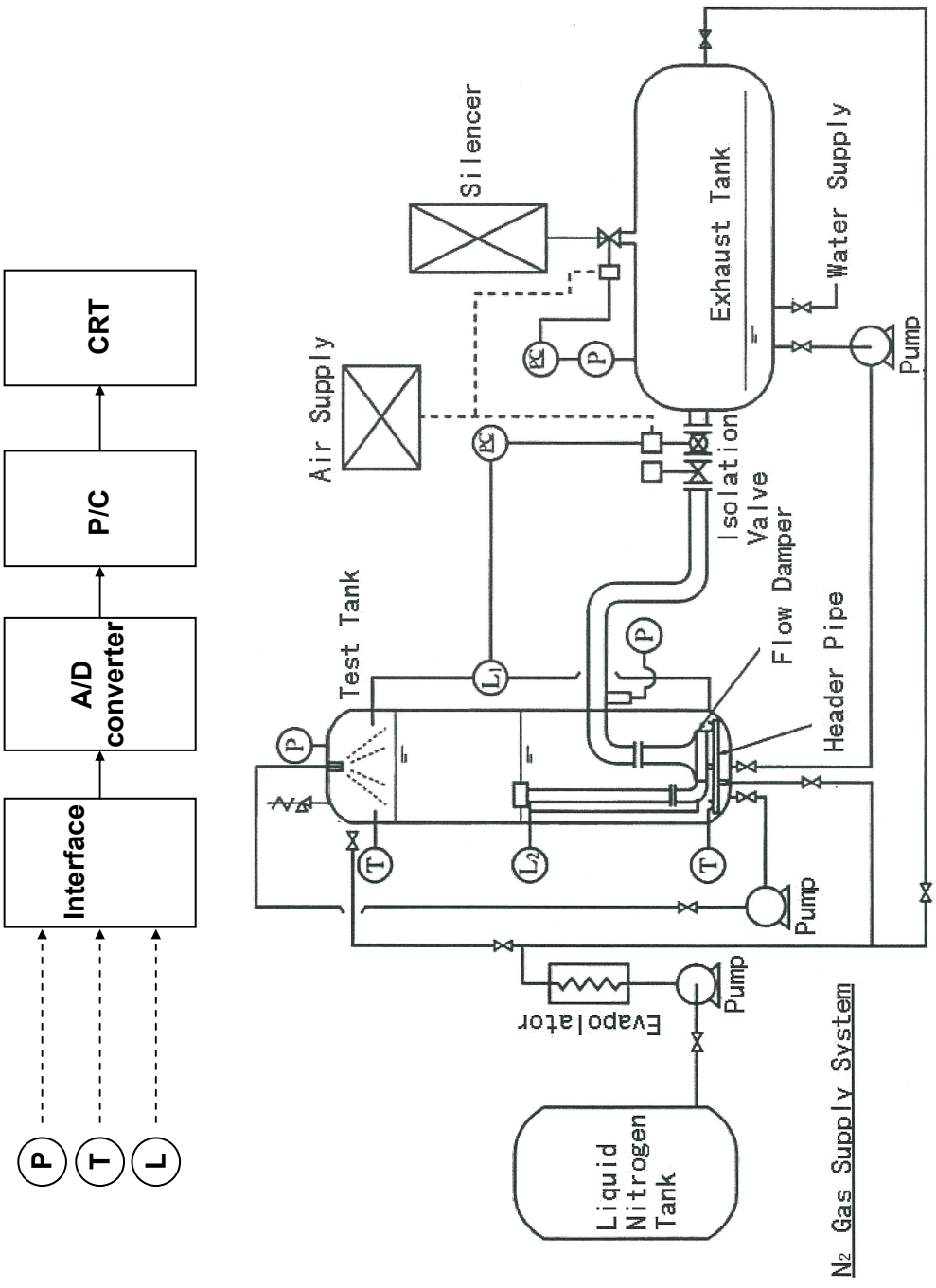

Fig. 4.2.4-1 Schematic Drawing of the Full Height 1/2 Scale Test Facility

Fig. 4.2.4-2 Outline Drawing of the Full Height 1/2 Scale Test Facility

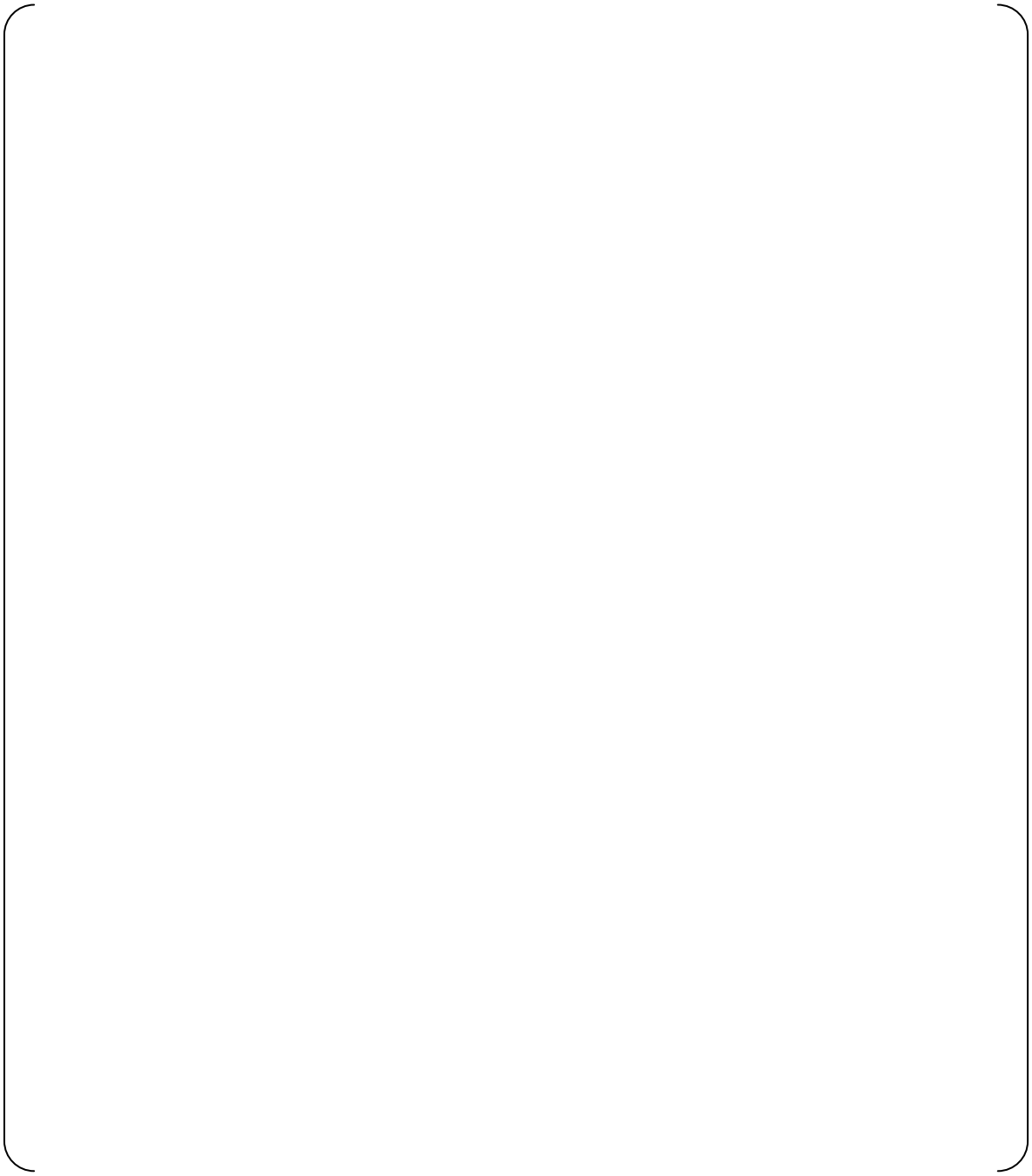

Fig. 4.2.4-3 Schematic Comparison of Actual Tank and Test Tank

Fig. 4.2.4-4 Outline Drawings of the Actual Flow Damper and the Test Flow Damper

3) Test Conditions

Full height 1/2 scale test conditions are shown in Table 4.2.4-1. The following seven cases were tested on initial tank pressure that reflects the ACC operating conditions. And the pressure of the exhaust tank corresponds to RCS pressure.

- Case 1: The initial test tank pressure was 586psig (4.04MPa [gage]) simulating the condition for ECCS performance during a large LOCA.
- Case 2: The initial test tank pressure was 657psig (4.53MPa [gage]) to obtain data for high pressure design.
- Case 3: The initial tank pressure was 758psig (5.23MPa [gage]) to obtain data for high pressure design.
- The pressure in the exhaust tank was 14psig (0.098MPa [gage]) for Case 1, 2, and 3. Since the pressure of the exhaust tank becomes the same as the pressure of the containment vessel (C/V) after the blow down phase during a large LOCA, and ECCS performance analysis uses approximately 14psig(0.098MPa [gage]), the pressure of the backpressure was set at 14psig (0.098MPa [gage]).
- Case 4: The initial tank pressure was the same as Case 1. However, the pressure in the exhaust tank was maintained at 71psig (0.49MPa [gage]) to obtain data for high back pressure.
- Case 5: The test was conducted with water containing dissolved nitrogen to confirm the effect of dissolved nitrogen gas on flow characteristics.
- Case 6: The test was conducted with a small differential pressure between the test tank and the exhaust tank to take into account large cavitation factors.
- Case 7: The injection test was conducted with the initial tank pressure was( ) ( ) assuming the pre-operational test condition.
- The valve opening speed was set at( ) seconds which is faster than the depressurization time during a LOCA in order to assure smaller cavitation factors.
- The resistance coefficient of the piping was controlled at the actual design condition( ) in order to confirm the injection time during the large flow injection period.

Table 4.2.4-1 Test Conditions of Full Height 1/2 Scale Test

	Test Tank Pressure	Exhaust Tank Pressure	Initial Gas Volume	Injection Water Volume		Objective
				Large Flow	Small Flow	
	psig [MPa [gage]]	psig [MPa [gage]]	ft^3 [m^3]	ft^3 [m^3]	ft^3 [m^3]	
Case 1	586 (4.04)	14 (0.098)	[redacted]			Obtain flow characteristics for ECCS performance evaluation during a large LOCA
Case 2	657 (4.53)	14 (0.098)				Obtain flow characteristics for high pressure design
Case 3	758 (5.23)	14 (0.098)				Obtain flow characteristics for large differential pressure
Case 4	586 (4.04)	71 (0.49)				Obtain flow characteristics for small differential pressure
Case 5	[redacted]					Obtain flow characteristics to confirm the effect of dissolved nitrogen gas
Case 6						Obtain flow characteristics in large cavitation factors
Case 7						Obtain flow characteristics for the assumed pre-operational test condition

4) Parameters and Measuring Equipment

Pressure, water level, and temperature were measured by the instruments shown in Fig.4.2.4-1 for all test cases and used to calculate the cavitation factor and the flow rate coefficient.

5) Test Results and Conditions

The test results are shown in Figs. 4.2.4-5 to 4.2.4-11. The test results, such as injection flow rate, test tank pressure, test tank water level and the flow rate coefficients [Note] during both large and small flow for each test case, are shown in these figures. The conclusions for each test are shown as follows.

Note: Where possible steady conditions were plotted.

[Case 1]

- It was confirmed that the injection flow rate was switched from large flow to small flow smoothly, and small injection began after large flow injection.[Refer to Fig.4.2.4-5(1/2)]
- It was confirmed that the test tank pressure dropped quickly after initiating the test and dropped gradually, after the flow rate switching at about approximately 114psig (0.8MPa [gage]). [Refer to Fig.4.2.4-5(2/2)]
- It was confirmed that when the test tank water level was reduced to the flow switching level, the standpipe water level temporarily dropped to its low point level in about 1.7 seconds and then recovered and continued to drop gradually during the small flow injection period. [Refer to Fig.4.2.4-5(1/2)]
- It was confirmed that the standpipe water level did not decrease to the top of the flow damper during flow switching. [Refer to Fig.4.2.4-5(1/2)]

[Case 2]

- Although the initial test tank pressure was 71psi (0.49MPa) higher than in Case 1, it was confirmed that the injection flow rate, test tank pressure and water level as a function of time were the same as in Case 1. [Refer to Fig.4.2.4-6(1/2), (2/2)]
- Since the initial test tank pressure was 71psi (0.49MPa) higher than in Case 1, the range of the cavitation factor during large flow shifted slightly to lower side. However, the flow rate coefficient was the same as in Case 1 in the region where the cavitation factor was the same as in Case 1. Therefore, it was confirmed that the characteristics of the flow rate coefficient and the cavitation factor are the same even if the tank pressure was increased 71psi (0.49MPa). [Refer to Fig.4.2.4-6(2/2)]
- It was confirmed that the characteristics of the flow rate coefficient and the cavitation factor during small flow were the same as in Case 1. [Refer to Fig.4.2.4-6 (2/2)]

[Case 3]

- Although the initial test tank pressure was 172psi (1.19MPa) higher than in Case 1, it was confirmed that the injection flow rate, test tank pressure and water level as a function of time were the same as in Case 1. [Refer to Fig.4.2.4-7(1/2), (2/2)]
- The flow rate coefficient was the same as in Case 1 in the performance range where the cavitation factor was the same as in Case 1. Therefore, it was confirmed that the characteristics of the flow rate coefficient and the cavitation factor are the same even if the tank pressure is increased by 172psi (1.19MPa). [Refer to Fig.4.2.4-7(2/2)]

- It was confirmed that the characteristics of the flow rate coefficient and the cavitation factor during small flow were the same as in Case 1. [Refer to Fig.4.2.4-7(2/2)]

[Case 4]

- Although the pressure of the exhaust tank was 71psig (0.49MPa [gage]) as opposed to 14psig (0.098MPa [gage]) in Case 1, it was confirmed that the injection flow rate, test tank pressure, and water level as a function of time were the same as in Case 1. [Refer to Fig.4.2.4-8(1/2), (2/2)]
- The flow characteristics data was obtained over a larger range of cavitation factors than Case 1 because of higher backpressure tank pressure. [Refer to Fig.4.2.4-8(2/2)]

[Case 5]

- For this case, Nitrogen gas was dissolved into the water. It was confirmed that the flow rate coefficient during large flow was smaller than that of the case where nitrogen was not dissolved. [Refer to Fig.4.2.4-9 (2/2)]
- It was confirmed that the flow rate coefficient during small flow was essentially the same as in Case 1 and no change was caused by the dissolved nitrogen gas. [Refer to Fig.4.2.4-9(2/2)]

[Case 6]

- It was confirmed that the injection flow rate was switched from large flow to small flow smoothly, and small injection began after large flow injection. [Refer to Fig.4.2.4-10(1/2)]
- The flow characteristics data was obtained for a larger range of cavitation factors than in Case 1 since the initial test tank pressure was reduced. [Refer to Fig.4.2.4-10(2/2)]

[Case 7]

- Although Case 7 was a low-pressure injection test, it was confirmed that the test tank pressure and water level were reduced rapidly during large flow and that the flow rate switching to small flow reduced gradually, as in Case 1. [Refer to Fig.4.2.4-11(1/2)]
- It was confirmed that the flow characteristics of the flow damper during both large and small flow were consistent with those in other cases. [Refer to Fig.4.2.4-11 (2/2)]

Performance Confirmation during Large Flow

In the case that simulates LOCA conditions, the resistance coefficient during large flow injection is less than[ ]. These results are generally consistent with the performance requirements.

Performance Confirmation during Small Flow

Measurements from the test results of Case 1 show that the flow rate before and after the flow switching was approximately 3170gpm (approximately 720m3/h) and approximately 652gpm (approximately 148m3/h), respectively. Therefore, the flow-switching ratio (3170/652=4.9) was less than[ ]and was consistent with the performance requirements.

Flow Switching Water Level

The measured flow-switching water level in each test case is shown in Table 4.2.4-2. The expected flow-switching water level was set at the lower end of the anti-vortex cap installed at the inlet of the standpipe. The actual flow-switching water levels were within the range from[ ]to[ ]of the expected flow switching water level.

Based on above test results, it was confirmed that the variation of flow-switching water level was limited to a sufficiently small range by the anti-vortex cap at the inlet of the standpipe.

Table 4.2.4-2 Flow Switching Water Level

	Initial tank pressure [psig (MPa [gage])]	Exhaust tank pressure [psig (MPa [gage])]	Flow switching water level [in (mm)][Note]
Case 1	586 (4.04)	14 (0.098)	
Case 2	657 (4.53)	14 (0.098)	
Case 3	758 (5.23)	14 (0.098)	
Case 4	586 (4.04)	71 (0.49)	
Case 5			
Case 6			
Case 7			

Note: Reference point is bottom of anti-vortex cap. The upper is '+', and the lower is '-'.

Water Level Reduction in Switching Flow Rate

It was confirmed that the reduction of the water level in each test during flow switching was smaller than the height of the standpipe and sufficient margin was provided to prevent gas entrainment. [Refer to Fig. 4.2.4-12]

Effect of Dissolved Nitrogen Gas

It was confirmed that, in the test with nitrogen saturated water (Case 5), the duration of large flow injection was slightly longer (approximately〔 〕) than in Case 1. Since Case 5 was conducted with nitrogen-saturated water, and this condition was not applicable in the actual accumulator tank, it is assumed that dissolved nitrogen is less effective in the actual tank. [Refer to Fig.4.2.4-9(2/2)]

Result of the Test Assuming Pre-operational Test Condition

The comparison between the characteristics of cavitation factor vs. flow rate coefficient measured in a LOCA simulation test (Case 1) and in this test is shown in Fig. 4.2.4-11. This comparison shows that the cavitation factor over a wide range can be obtained from this test and beyond the results of LOCA simulation test (Case 1). [Refer to Fig.4.2.4-11(2/2)]

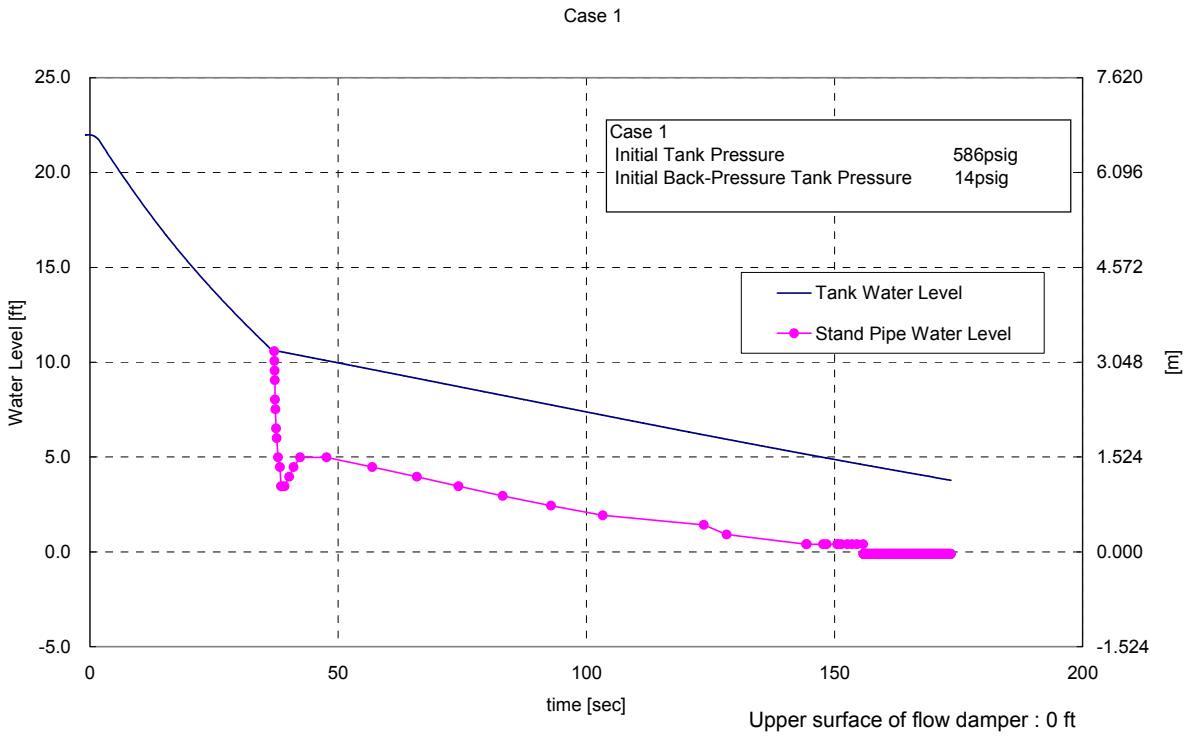

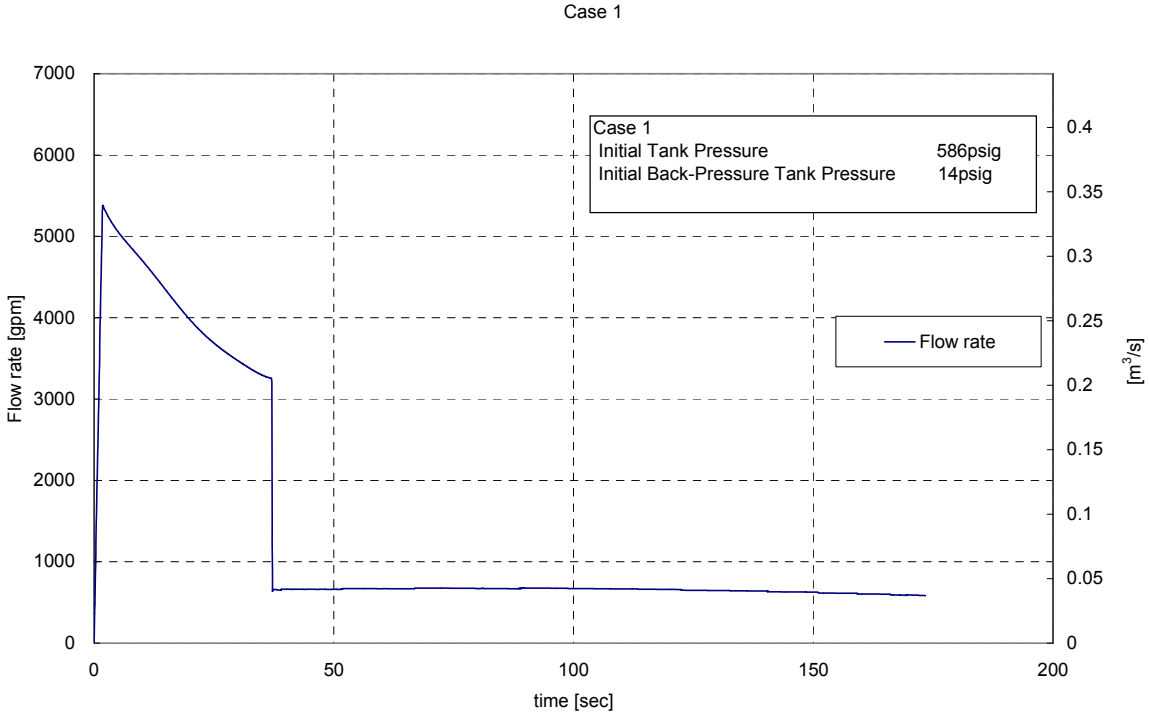

Fig. 4.2.4-5 (1/2) Full Height 1/2 Scale Test Results (Case 1) 1/2

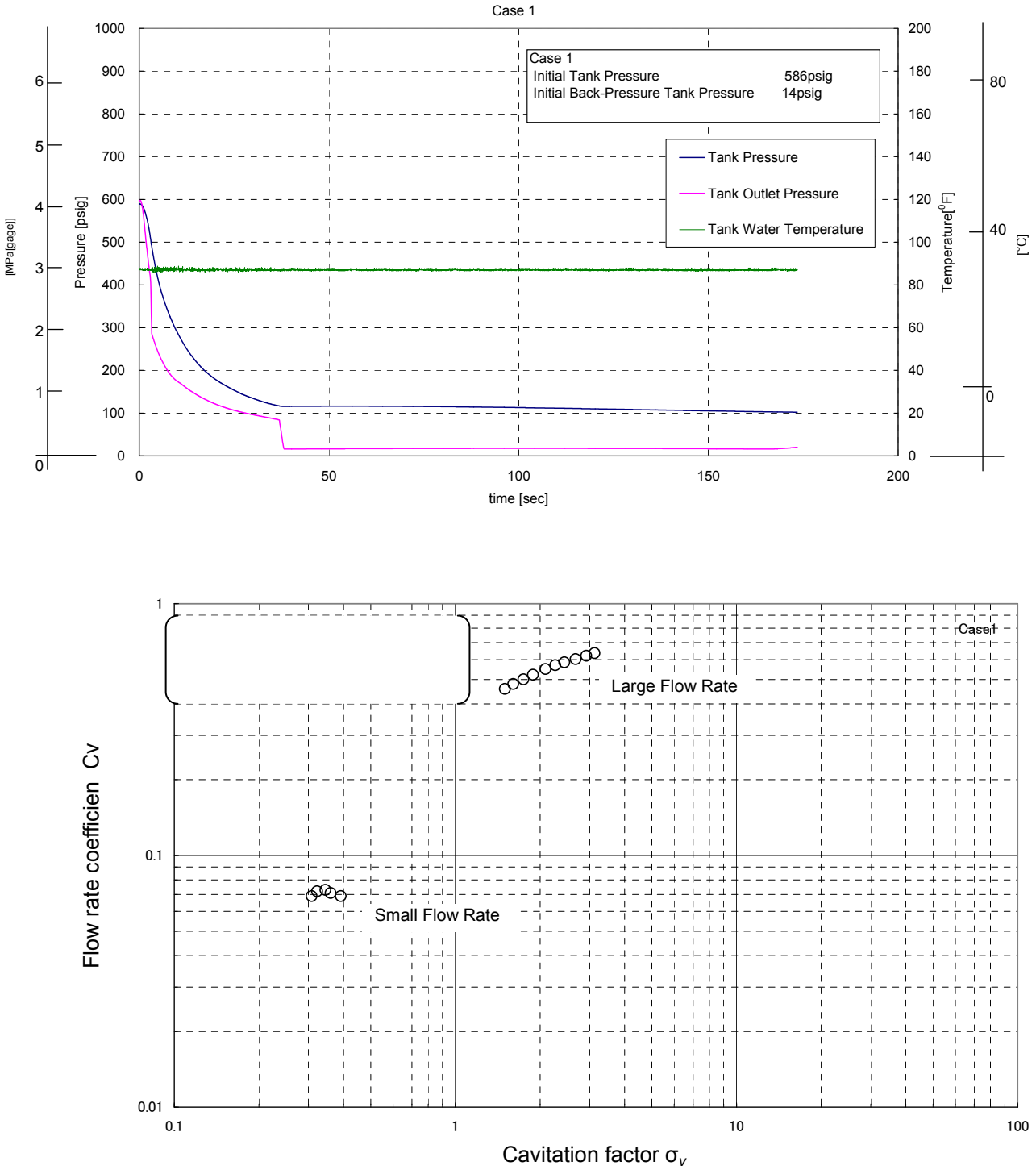

Fig. 4.2.4-5 (2/2) Full Height 1/2 Scale Test Results (Case 1) 2/2

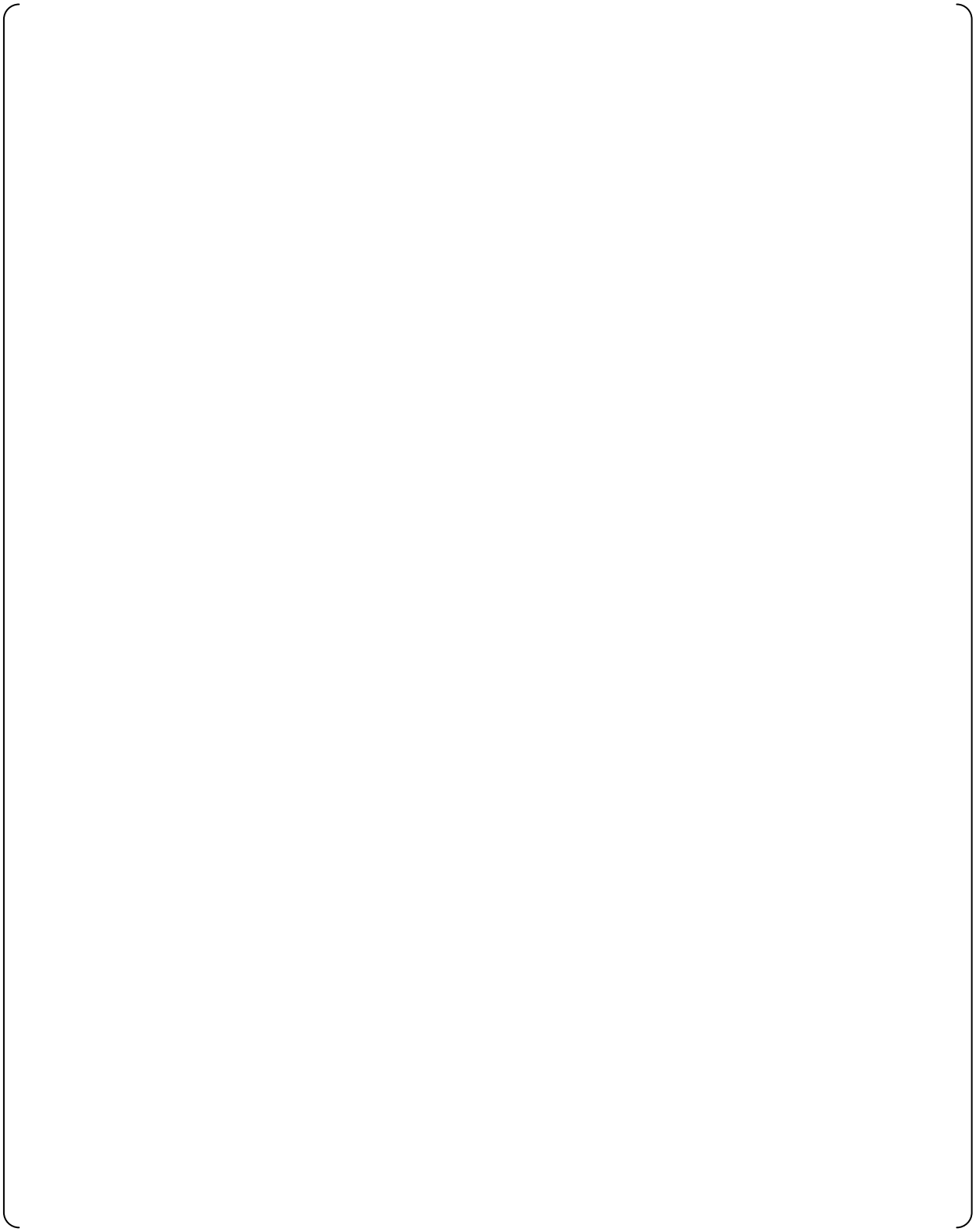

Fig. 4.2.4-6 (1/2) Full Height 1/2 Scale Test Results (Case 2) 1/2

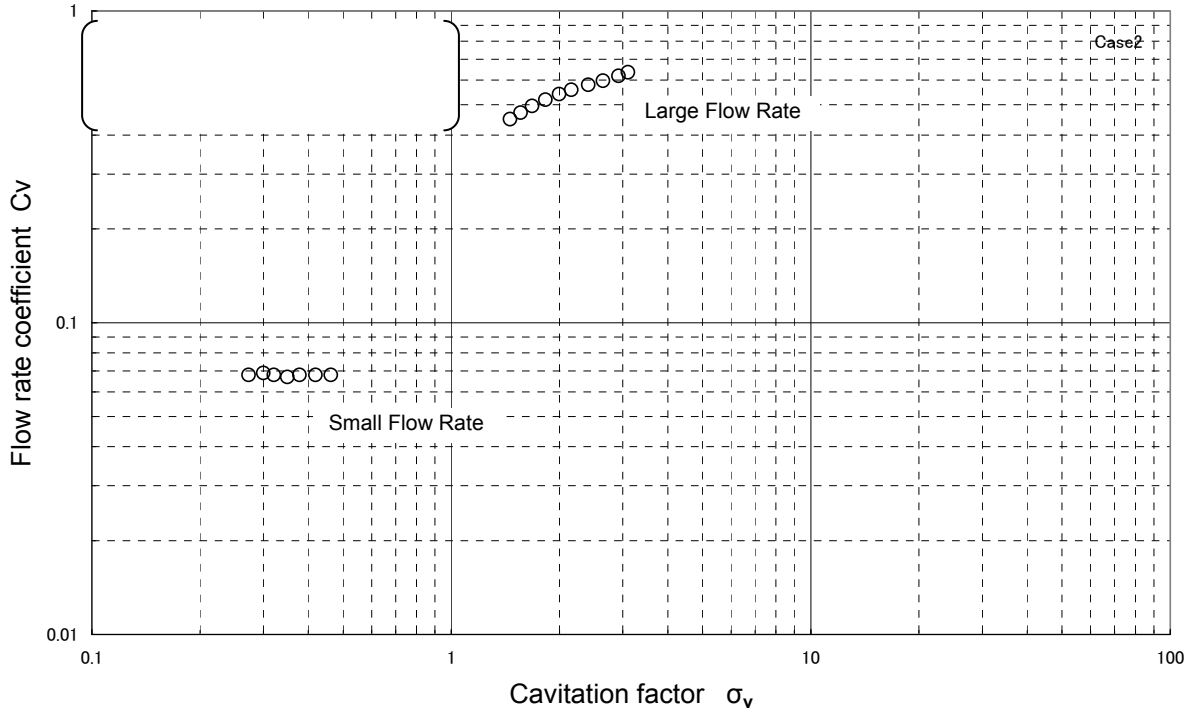

Fig. 4.2.4-6 (2/2) Full Height 1/2 Scale Test Results (Case 2) 2/2

Fig. 4.2.4-7 (1/2) Full Height 1/2 Scale Test Results (Case 3) 1/2

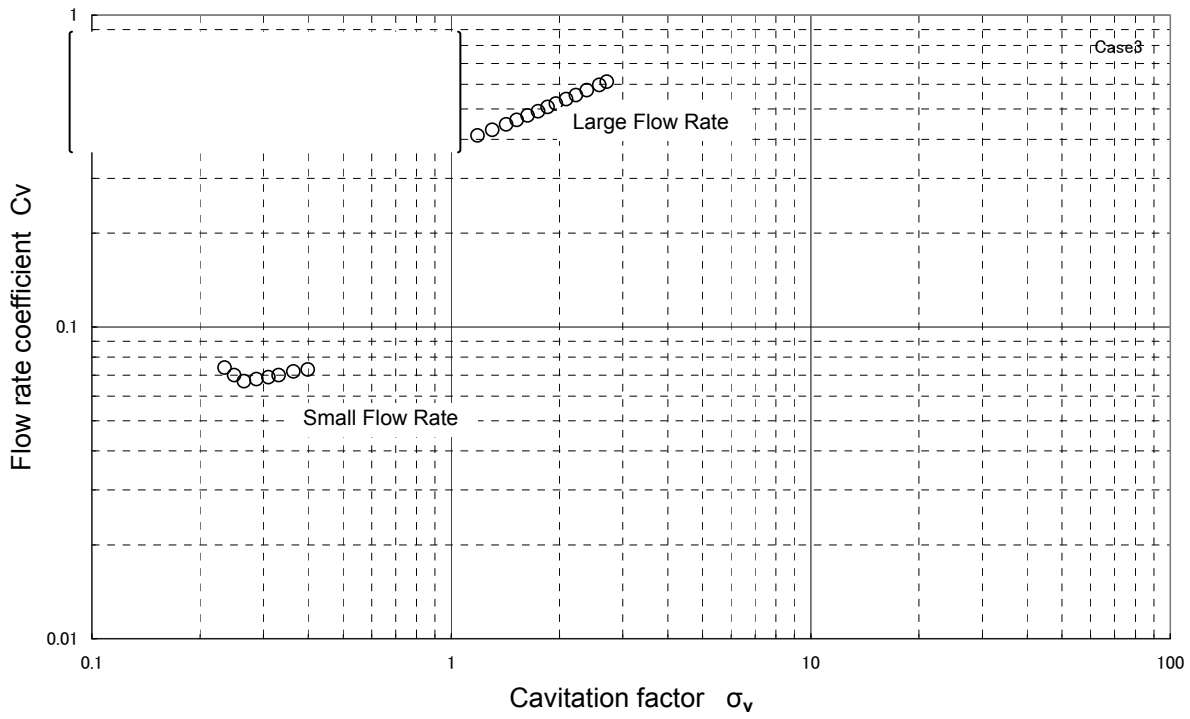

Fig. 4.2.4-7(2/2) Full Height 1/2 Scale Test Results (Case 3) 2/2

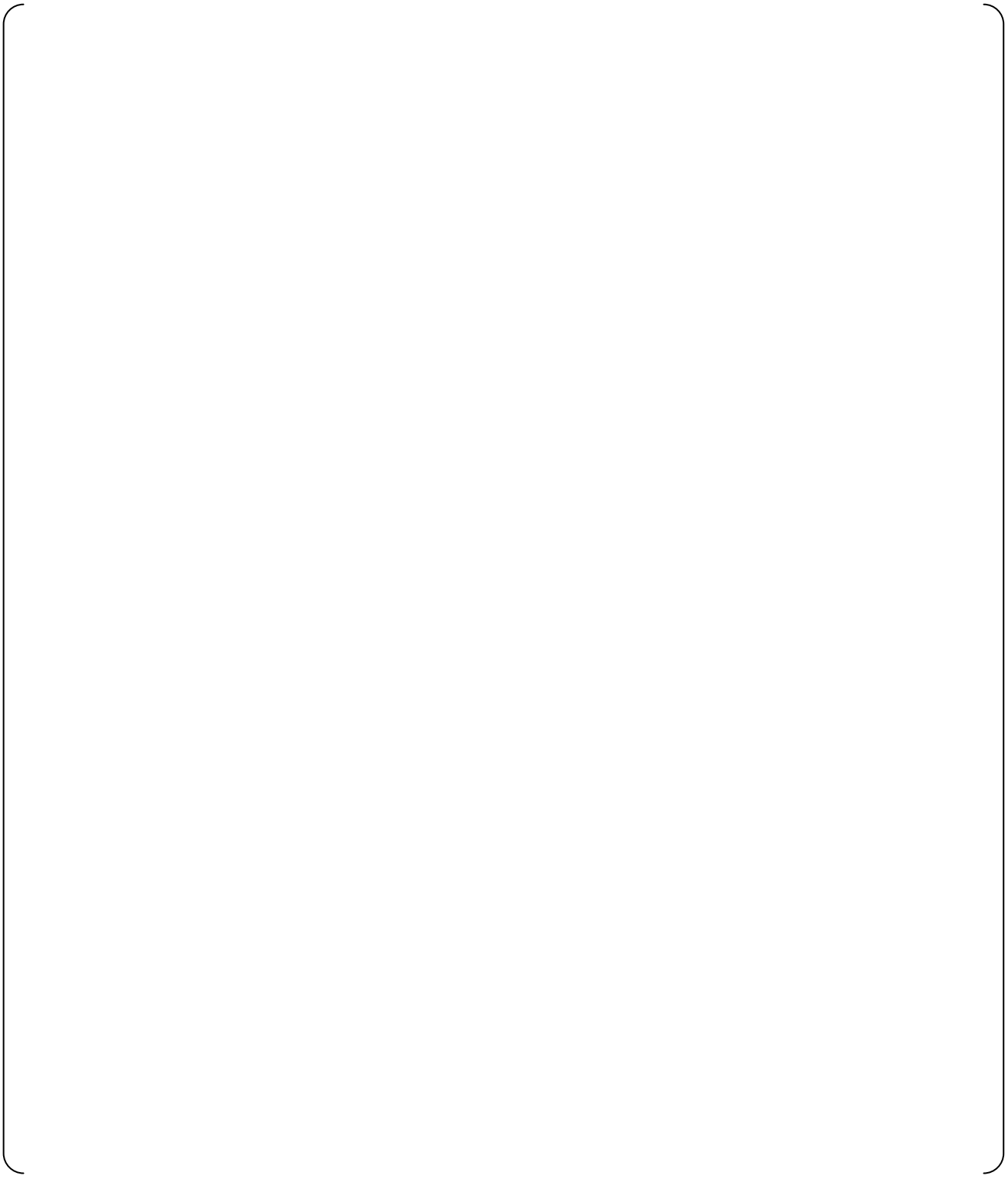

Fig. 4.2.4-8 (1/2) Full Height 1/2 Scale Test Results (Case 4) 1/2

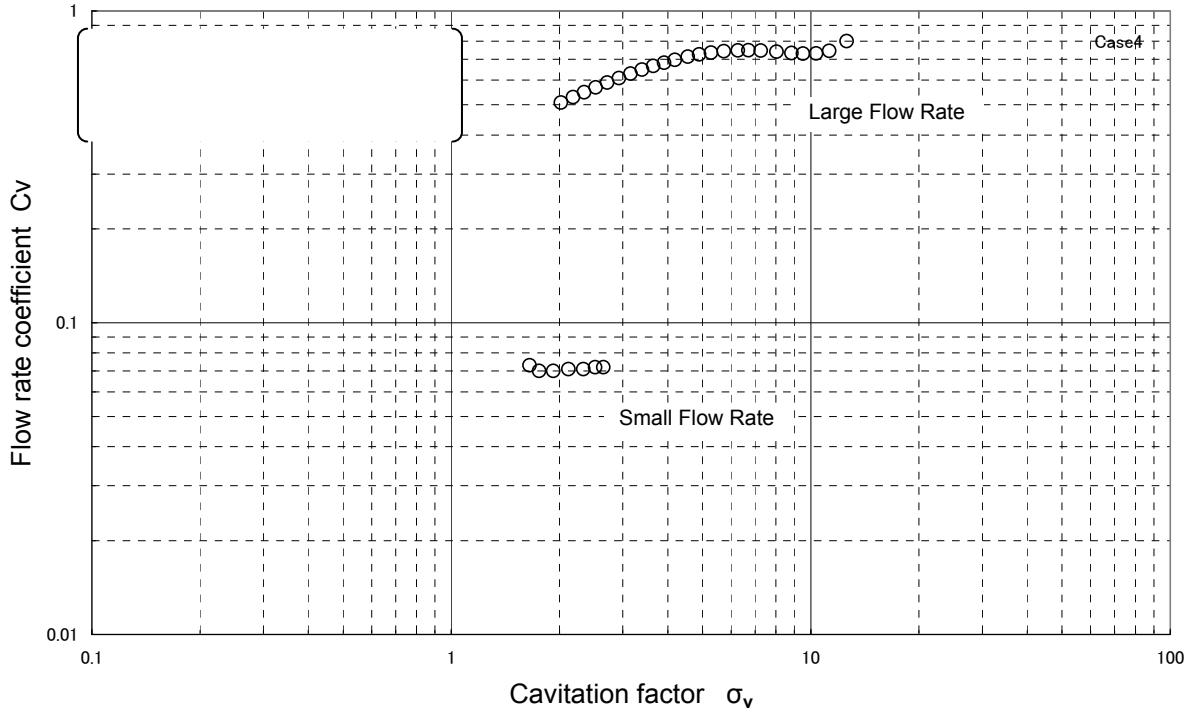

Fig. 4.2.4-8 (2/2) Full Height 1/2 Scale Test Results (Case 4) 2/2

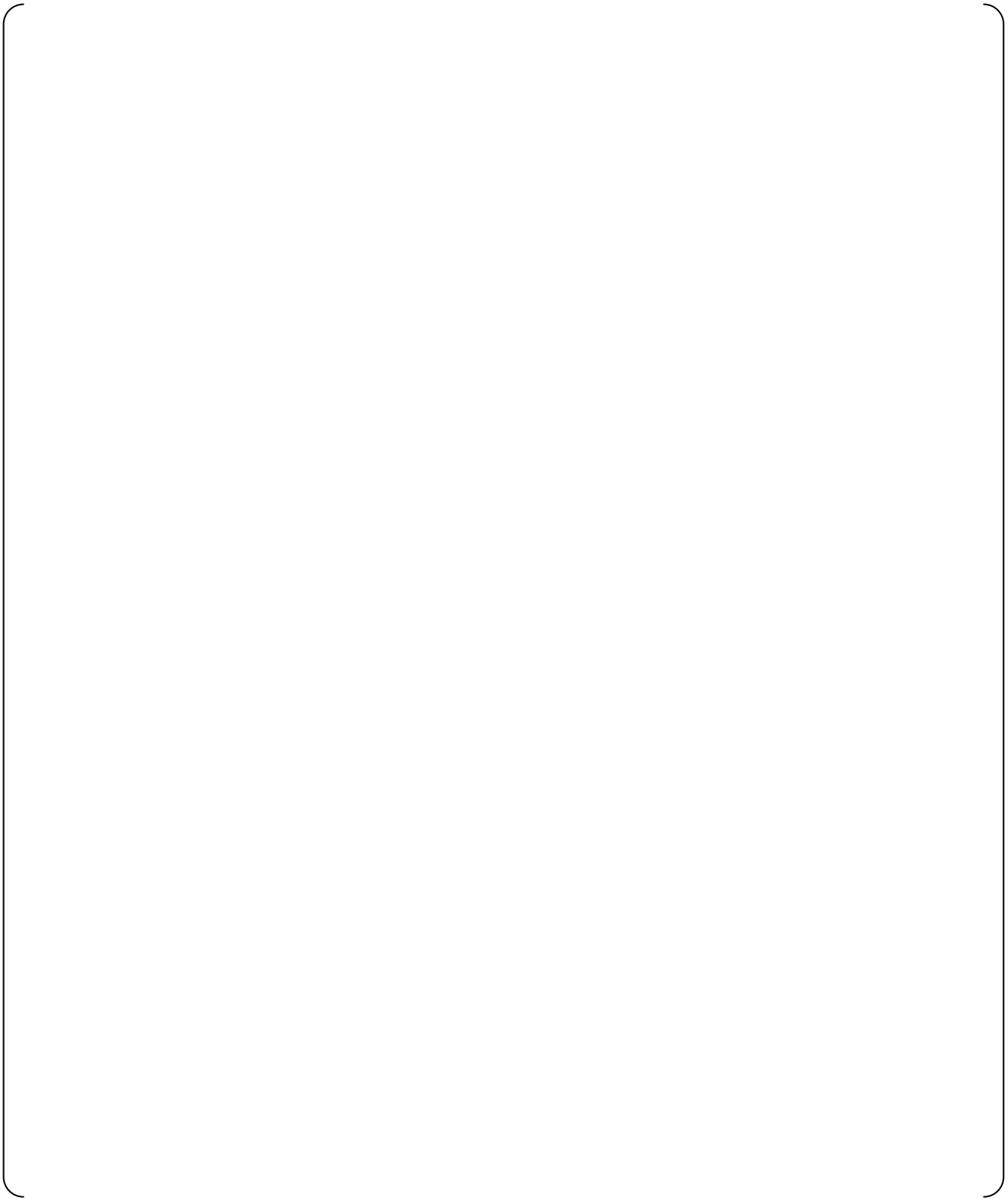

Fig. 4.2.4-9 (1/2) Full Height 1/2 Scale Test Results (Case 5) 1/2

Fig. 4.2.4-9 (2/2) Full Height 1/2 Scale Test Results (Case 5) 2/2

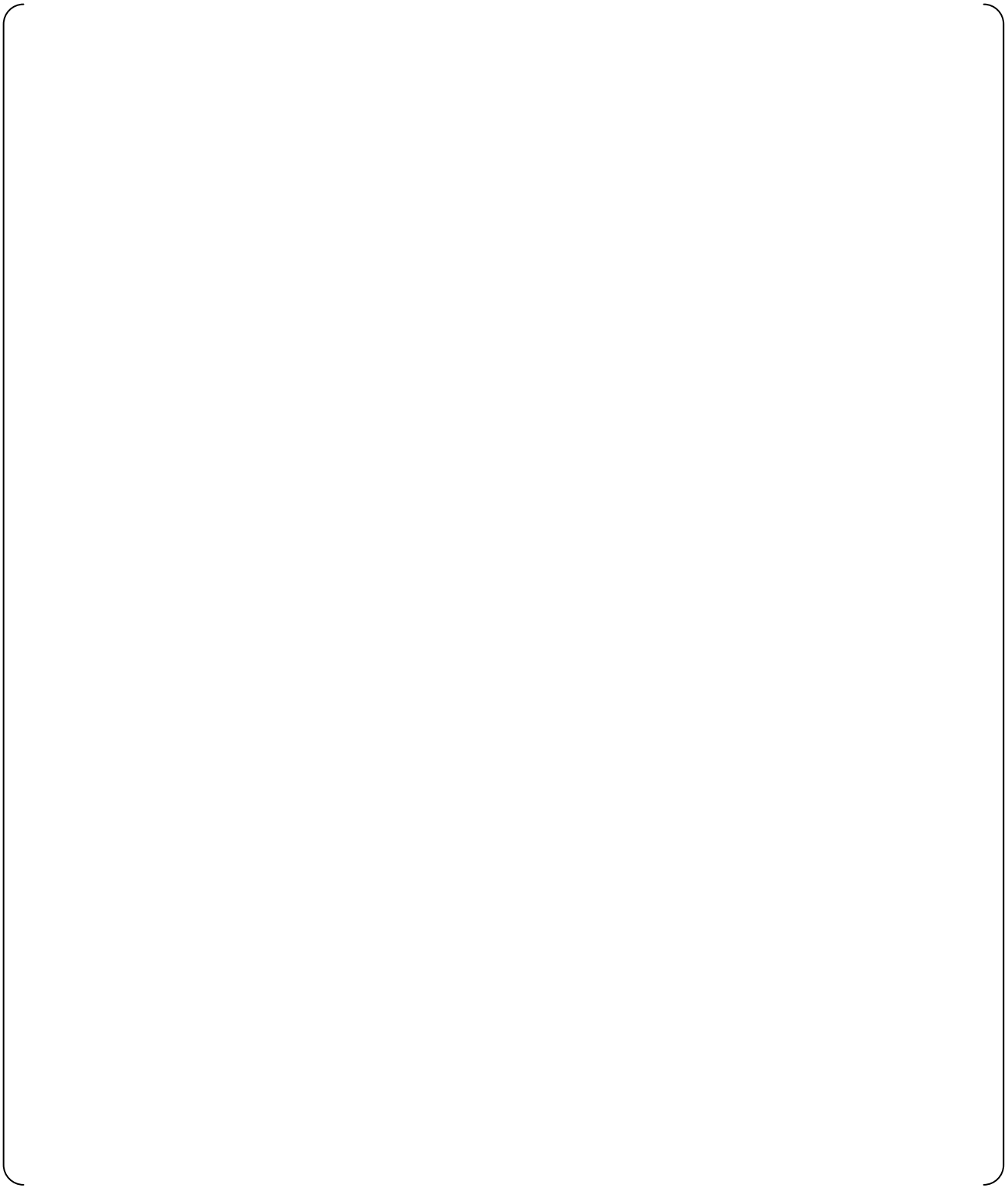

Fig. 4.2.4-10 (1/2) Full Height 1/2 Scale Test Results (Case 6) 1/2

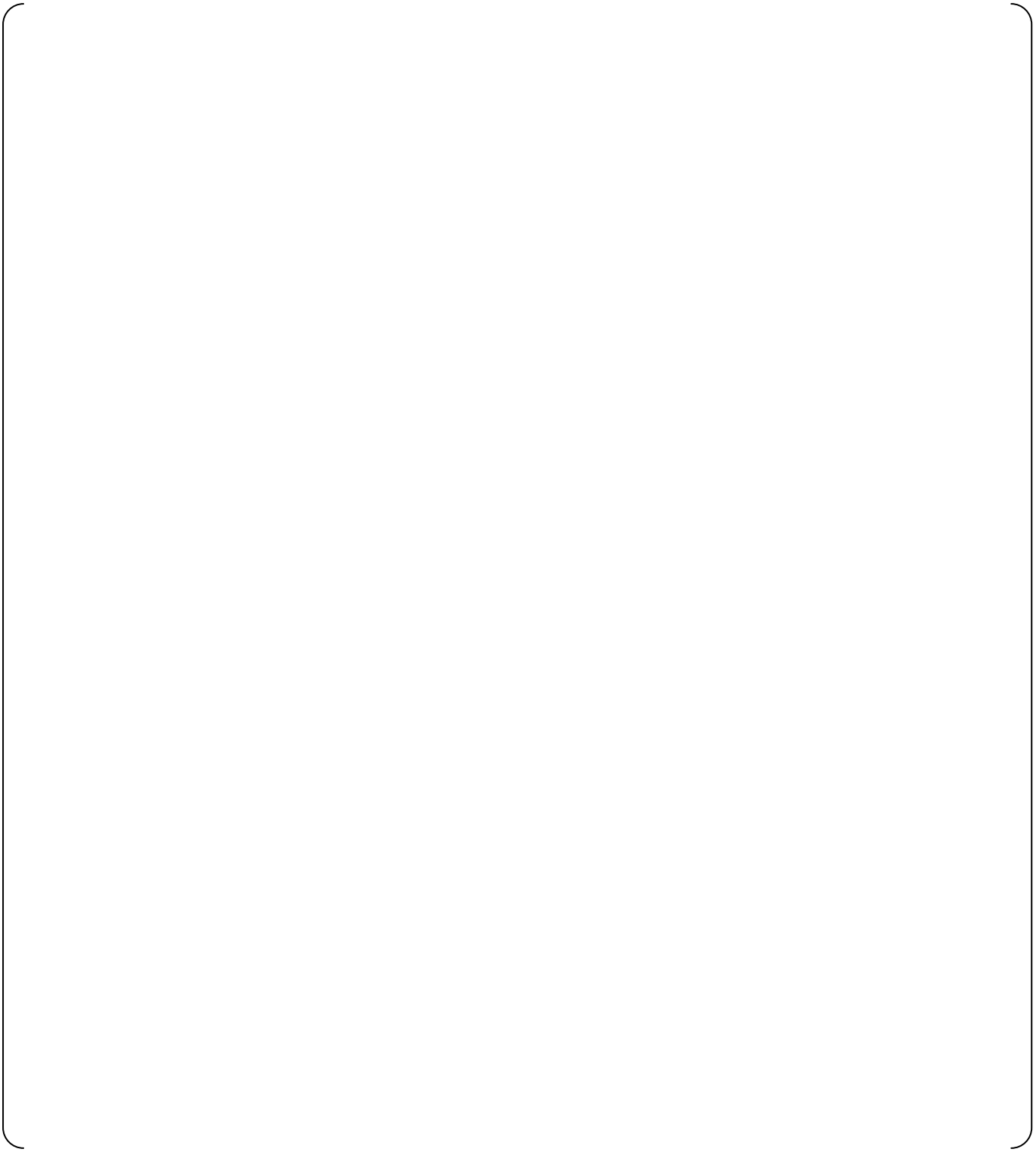

Fig. 4.2.4-10 (2/2) Full Height 1/2 Scale Test Results (Case 6) 2/2

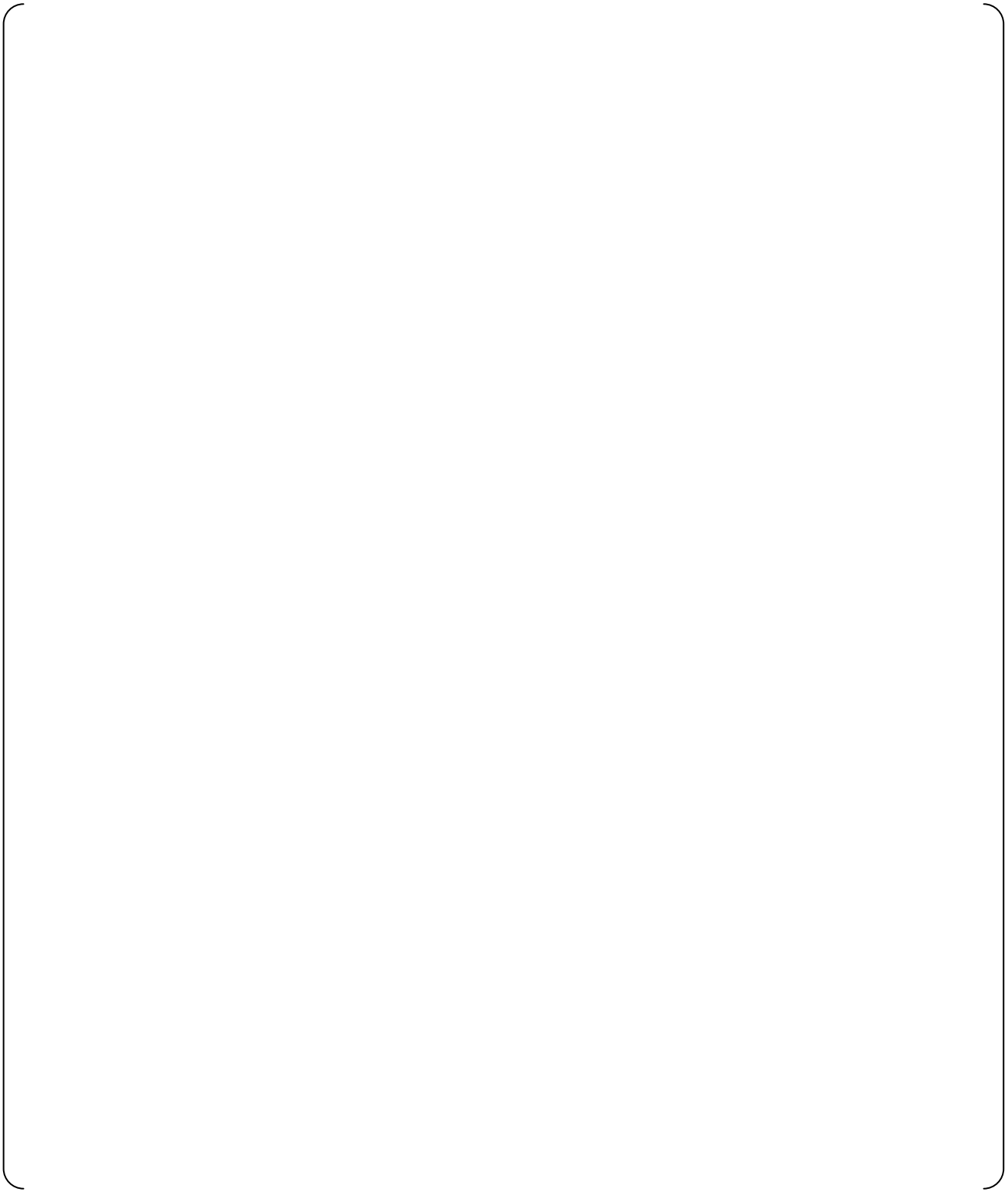

Fig. 4.2.4-11(1/2) Full Height 1/2 Scale Test Results (Case 7) 1/2

Fig. 4.2.4-11(2/2) Full Height 1/2 Scale Test Results (Case 7) 2/2

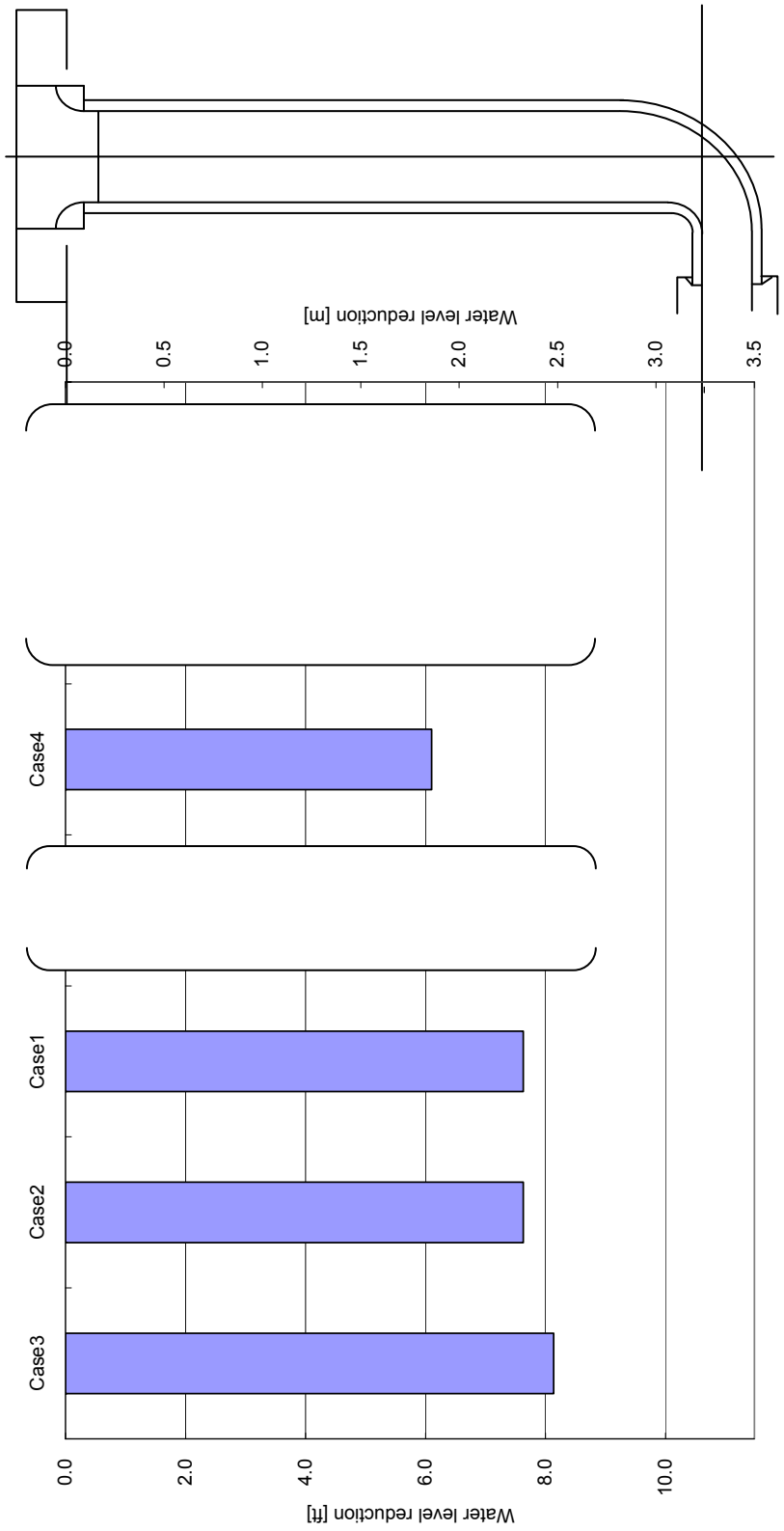

Fig. 4.2.4-12 The Test Results of Water Level Reduction in Switching Flow Rate

4.3 Validity and Scalability of Flow Rate Characteristics

The governing equations of flow in the flow damper are the equation of continuity and the Navier-Stokes equation for incompressible flow. The dimensionless forms of these equations and the boundary conditions of the flow damper give two dimensionless numbers: a Reynolds number for internal flow and a Froude number for a free surface. Therefore, a Reynolds number will affect the resistance of the internal flow in the flow damper without cavitation, while a Froude number will affect the behavior of the free surfaces in the accumulator tank and the standpipe.

Since cavitation bubbles may reduce the flow rate, a cavitation factor is another parameter that affects the flow resistance of the flow damper in addition to the Reynolds number. Generally speaking, friction coefficients come to a constant as the Reynolds number gets larger. If the effect of friction can be neglected at a large Reynolds number, cavitation factor will be the only parameter of the flow rate coefficient.

Table 4.3-1 shows the Reynolds numbers for the 1/5-scale model, the full height 1/2-scale model and the actual plant. This table shows that each the Reynolds number is generally large enough that the effect of friction can be neglected.

Fig.4.3-1 shows the flow rate coefficient with respect to cavitation factors obtained by the 1/5-scale and full height 1/2-scale models of the flow damper. There are two lines: one for the large flow rate injection and the other for the small flow rate injection. The data for both 1/5-scale and full height 1/2-scale models collapsed into the same lines for large and small flow rates from which in fact.

Consequently, the flow rate characteristics with respect to cavitation factor shown in Fig. 4.3-1 are the flow characteristics applicable to the actual ACC.

Table 4.3-1 Comparison of Reynolds number

	Reynolds Number
Actual Plant	
Full height 1/2-scale model	
1/5-scale model	

Note: Reynolds numbers are calculated with respect to the throat.

Fig. 4.3-1 Flow Rate Coefficient with Respect to Cavitation Factor of the Flow Damper for Full Height 1/2 Scale and 1/5 Scale Models

The trend that the flow rate coefficient lessens as the cavitation factor gets smaller for the large flow rate injection is reasonable, because cavitation is stronger for a smaller cavitation factor. And the flow rate coefficient approaches a constant value as the cavitation factor gets larger, because cavitation is reduced and vanishes for larger cavitation factors.

Since there is no cavitation at the throat for the small flow rate injection, the flow rate coefficient for small flow should be independent of a cavitation parameter as shown in Fig. 4.3-1.

In case of the full height 1/2 scale model, the accumulator tank with the same height and the same nitrogen-gas pressure as those of the actual ACC gives the same Froude number as that of the actual ACC for a given backpressure, or RCS pressure. It simulates the same transients of injection velocity, water level in the standpipe, and pressures in the test apparatus as those of the actual ACC. We can thus confirm the injection of cooling water at the actual conditions with that of the full height 1/2 scale model.

The performance of the actual accumulator will be confirmed in a pre-operational test.

4.4 Quality Assurance of the ACC Test Program

1) General

The results of the ACC test program, performed from June 1994 to August 1996, are applicable to the US-APWR. These results were reviewed and MHI confirmed that the requirements of the Japanese QA Guideline and QA activities at that time met the requirements of 10 CFR 50 Appendix B and ASME NQA-1-1994, by comparing the requirements of the Japanese QA Guideline to those of 10 CFR 50 Appendix B and ASME NQA-1-1994.

2) Procedure of Re-verification

The ACC test program was re-verified and confirmed to be reliable and accurate for use in the US-APWR. This re-verification was performed by evaluating the following items in accordance with a written procedure.

(1) Confirmation of Test Procedure
(2) Evaluation of Test Personnel
(3) Evaluation of Test Equipment
(4) Evaluation of Test Procedure (execution)
(5) Evaluation of Test Results
(6) Evaluation of Design Personnel Concerning to the Test

3) Results

It was confirmed that the reliability and accuracy for the ACC test program satisfied the requirements of 10 CFR 50 Appendix B and ASME NQA-1-1994.

The following sets out the re-verification results of the above six items.

(1) Confirmation of Test Procedure

The ACC test program can be applied to the US-APWR by comparing the test conditions as follows:

- MHI established test conditions for the ACC of the US-APWR consistent with the design requirements for the ACC of the US-APWR.
- MHI compared the previous APWR test conditions with the test conditions established for the US-APWR and confirmed that the previous test conditions are applicable to the US-APWR.
- The test conditions that were compared and confirmed were the following prerequisite conditions for the test:
- Prerequisites: - Adverse conditions (considering operating modes and environments)
  - Configuration
  - Test scope addressed applicable design features

(2) Evaluation of Test Personnel

It was confirmed that the test personnel who had conducted the previous tests satisfied the current necessary qualifications as follows:

- MHI reviewed the qualifications of the test personnel who had conducted the previous tests against current qualification requirements (NQA-1-1994 2S-1).
- MHI established records documenting this re-verification of the qualifications of the testing personnel.

(3) Evaluation of Test Equipment

It was confirmed that the condition and the accuracy of the test equipment and measurements used during the testing met current requirements taking into account the test objectives for the US-APWR. The results of this validation were as follows:

- MHI documented the test objectives and test results required for the US-APWR based on the design conditions for the ACC of the APWR.
- Based on this document, MHI established the requirements for the accuracy of test equipment and measurements for the US-APWR.
- MHI determined that the accuracy of the test equipment and measurements used in the ACC test program at that time satisfied the requirements for the US-APWR.

(4) Evaluation of Test Procedure (execution)

It was confirmed that the test procedure used for conducting the ACC tests at that time meets the current requirements as follows:

- MHI documented the design requirements for the US-APWR (i.e., items that must be verified in the test) based on the design conditions for the ACC as used in the US-APWR.
- MHI confirmed that the test procedure used at that time the tests were conducted meets the present requirements and are appropriate by comparing the items that were to be verified by those tests with the above identified design requirements for the US-APWR to be verified by test.

(5) Evaluation of Test Results

Test results were evaluated by the responsible design organization and it was confirmed that the test results obtained could be applied to the US-APWR.

- MHI documented this evaluation of the applicability of the past test results to the US-APWR.

(6) Evaluation of Design Personnel Concerning to the Test

Design personnel responsible for the test at that time had participated in the test process from the commencement of test preparations (e.g. test plan, test procedure, test equipments) to the completion of the tests and had both witnessed and evaluated the test results. MHI also confirmed that design test program was independently reviewed by experienced engineers and the tests were witnessed by representatives of the funding the design personnel of utilities and MHI. Therefore, the test at that time was objective. MHI confirmed that the design personnel had participated in the design of the test plan, test procedure, and test equipment and also in the evaluation of test results from evidence such as meeting minutes, trip reports and document review reports etc.

- MHI confirmed based on meeting minutes, trip reports, etc. that meetings concerning the test plan, test procedure, and test equipment had been held with the utilities and that the designs had been reviewed by the utilities and their comments had been incorporated.
- MHI confirmed that the design personnel of utilities and MHI had witnessed the actual test.
- MHI confirmed that the design review (e.g. Design Review Board) for the overall review of the test, including the test plan, test procedure, test equipment, and test results, was conducted by independent experienced engineers.

5.0 CONCEPT OF THE SAFETY ANALYSIS MODEL

5.1 Characteristic Equations of Flow Rates for the Safety Analysis

The flow rate coefficient is a function of the cavitation factor as shown in Fig.5.1-1. Experimental formulae of the flow rate characteristics of the flow damper were derived with respect to a cavitation factor separately for the large and small flow rate injections each by curve fitting using the data of the full height 1/2-scale tests. The curve fitting is based on the least-squares method. An exponential function was chosen as the form of the fitting curves to give the best fitting of the data. The resultant experimental equations are:

$$C_v = 0.7787 - 0.6889\,exp\left(-0.5238\sigma_v\right) \quad \text{For Large Flow Rate Injection,} \qquad (5\text{-}1)$$

and

$$C_v = 0.07197 - 0.01904\,exp\left(-6.818\sigma_v\right) \quad \text{For Small Flow Rate Injection} \qquad (5\text{-}2)$$

The flow resistance coefficient of the flow damper (K_D) is given by

$$K_D = \frac{1}{C_v^{\,2}} \qquad (5\text{-}3)$$

Fig. 5.1-1 The Flow Characteristics of the Flow Damper

5.2 Estimation of Uncertainty of the Characteristic Equations of Flow Rates

The data from the full-height, full pressure, 1/2 diameter experiment was used to develop the characteristic equations for the ACC performance. Errors of measured values consist of experimental errors, instrument errors and manufacturing errors. The causes of experiment errors may be turbulence, unsteadiness of flow, structural vibration, noises, etc. The causes of instrument errors may be sensitivities of sensors, linearity of instruments, etc. The causes of manufacturing errors may come from machining and assembling accuracies.

The total error of a measured value was, however, divided into a bias error and a random error according to ANSI/ASME PTC19.1-1985 as described below. In LOCA analysis, uncertainty of characteristic equation will be considered conservatively to evaluate fuel cladding temperature using these errors.

Random Errors

Pressures and water levels were measured as a function of time. The raw data generally scatter and form a band with time. For LOCA analysis, it is necessary to use the reduced data without dispersion that represent the flow rate characteristics of the flow damper. These reduced data were taken by curve fitting of the raw data to make a curve that lies at the middle of the data band. The experimental equations were derived from the curves. The standard deviation of the dispersion of the data from the experimental equations was evaluated as random errors for each test case as shown in Table 5.2-1.

Table 5.2-1 Dispersion of the Data from the Experimental Equations

Instrument Uncertainties

A true value may be different from the experimental equations. This difference is defined as an experimental error. However, the true value is not known and needs to be estimated. Each string of a sensor, an amplifier, an A/D converter and a process computer was calibrated one by one. Instrument uncertainties consist of accuracy of each instrument string as a bias error and sampling error of each calibration as a random error and were calculated by root-sum-square of them. Instrument uncertainties associated with flow rate coefficients is shown for each test case in Table 5.2-2.

Table 5.2-2(1/2) Instrument Uncertainties at Large Flow

Table 5.2-2(2/2) Instrument Uncertainties at Small Flow

Manufacturing Errors

The manufacturing error of the flow damper associated with the flow rate coefficient is determined based on the dimensions and manufacturing tolerance of the following parts that affect the performance of the flow damper.

- The inner diameter of the throat
- The facing angle (collision angle) of the large flow inlet pipe and the small flow inlet pipe
- The inner diameter of the vortex chamber
- The width of the small flow pipe
- The height of the small flow pipe

Consequently, the manufacturing error associated with the flow rate coefficient will be less than( ).

5.3 Estimation of Potential Uncertainties of Water Level for Switching Flow Rates

The uncertainty in the switching levels as function of the water level in the test tank was taken from elevation data of the inlet port of standpipe in full height, full pressure, 1/2 diameter experiments. A water level at switching of flow rates was defined as an intersecting point of two curves of water levels for large flow rate injection and small flow rate injection. The instrument errors were also counted in the estimation of the uncertainties.

Uncertainty of water level for switching flow rates in each test case is shown in Table 5.3-1.

Table 5.3-1 Uncertainty of Water Level for Switching Flow Rates

5.4 LOCA Analytical Model and Computational Procedure

The resistance coefficient of the flow damper varies over time depending on the flow condition. The resistance coefficient is calculated by the correlation equations between cavitation factor and flow rate coefficient.

The correlation equations are incorporated into the LOCA analysis computer code and resistance coefficient of the flow damper is calculated at each time-step in the LOCA analysis. Compared with the ACC, the resistance coefficient of a conventional nuclear plant accumulator does not vary for conditions such as pressure and flow rate.

The computational procedure for determining the resistance coefficient of the ACC is determined as follows;

1) Calculate cavitation factor σ_v from the flow condition at the flow damper.

$$\sigma_v = \frac{P_D + P_{at} - P_v}{\left(P_A + \rho g H\right) - \left(P_D + \frac{\rho V_D^2}{2} + \rho g H'\right)} \tag{5-4}$$

Where,

σ_v	:	Cavitation factor
P_{at}	:	Atmospheric pressure
P_D	:	Flow damper outlet pressure [gage]
P_A	:	Gas pressure in accumulator
P_v	:	Vapor pressure
ρ	:	Density of water
g	:	Acceleration of gravity
H	:	Distance between ACC water level and vortex chamber
H'	:	Distance between outlet pipe and vortex chamber
V_D	:	Velocity of injection pipe

2) Calculate the flow rate coefficient *Cv* using the following correlations.

For large flow rate: $C_v = 0.7787 - 0.6889 \exp(-0.5238\ \sigma_v)$ (5-5)

For small flow rate: $C_v = 0.07197 - 0.01904 \exp(-6.818\ \sigma_v)$ (5-6)

The injection flow rate switches to small flow rate when the calculated accumulator water volume becomes less than the volume below the standpipe inlet level.

Uncertainty of characteristics equations is considered conservatively to evaluate fuel cladding temperature in LOCA analysis.

3) Convert flow rate coefficient C_v to resistance coefficient of the flow damper K_D.

$$K_D = \frac{1}{C_v^2} \tag{5-7}$$

4) Calculate total resistance coefficient by summing up resistance coefficient of the flow damper and that of injection piping.

$$K_{acc} = K_D + K_{pipe} \quad (5\text{-}8)$$

Where,

K_{acc} : Total resistance coefficient of the flow damper and injection piping

K_{pipe} : Total resistance coefficient of injection piping

6.0 SUMMARY

The Mitsubishi Heavy Industries, Ltd. Advanced Accumulator (ACC) design will be used in MHI's Advanced Pressurized Water Reactors. The ACC design simplifies the emergency core cooling system design by integrating the short term large flow rate design requirements currently satisfied in conventional pressurized water reactor designs by the combined injection capabilities of the primary system accumulator and the low head safety injection pump into a single passive device, the ACC.

The ACC is a borated water storage tank with a fluidic device that throttles the flow rate of cooling water injected into a reactor vessel from a large to a small flow rate. A conceptual drawing of the ACC is shown below.

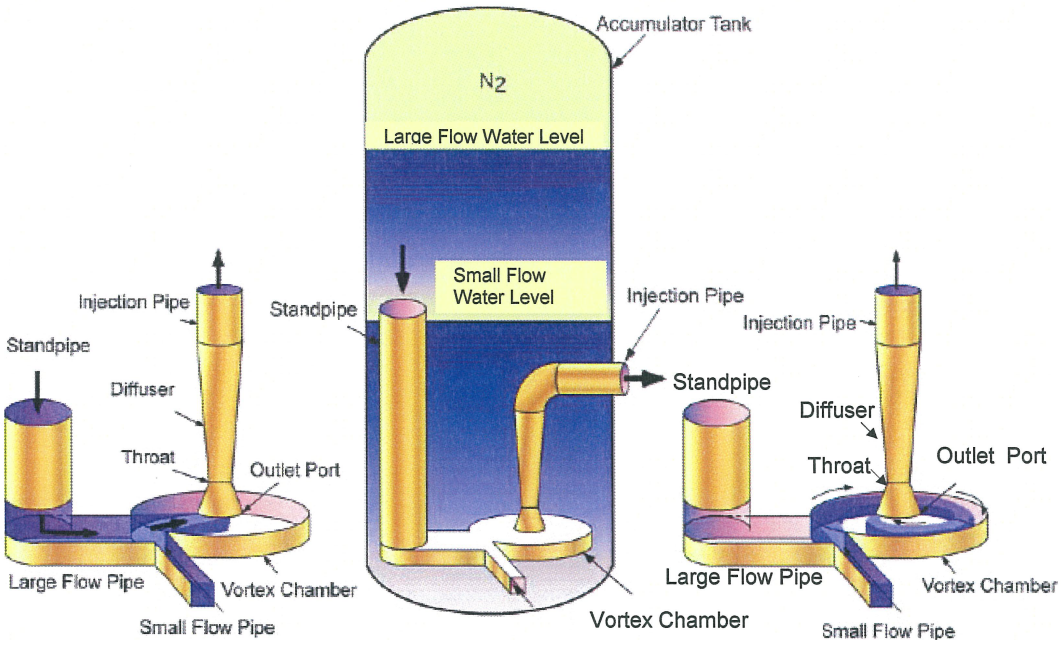

Large Flow (RV Refilling) **Water Levels in Accumulator Tank** **Small Flow (Core Reflooding)**

The vortex chamber at the inlet of the injection pipe in the accumulator tank accomplishes the flow rate throttling from large flow to small flow by establishing a vortex (and thus a large pressure drop) at a predetermined accumulator tank level. The inlet of the standpipe is located at the ACC volume level at which the transition from large to small flow is desired to occur. The ACC is a simple device that achieves precise throttling from a large injection flow rate to a small injection flow rate with no moving parts.

Upon initiation of a large break loss of coolant accident, all short term low head primary coolant injection flow requirements are satisfied by the ACC. Following depletion of the ACC water volume, the longer term ECCS flow requirements are met by the safety injection pumps thus eliminating the need for low head injection pumps. The immediate availability of low head flow provided by the ACC upon loss of electrical power coincident with a large break loss of coolant accident provides additional time for actuation of the backup emergency power source.

The design requirements and specifications of the ACC for the US-APWR are the same as that for the APWR. The confirmatory test program for the APWR was successfully conducted as a joint study among five utilities (Japan Atomic Power Co., Hokkaido Electric Power Co., Kansai Electric Power Co., Shikoku Electric Power Co., and Kyushu Electric Power Company) and MHI, from September 1994 to September 1996. The tests confirmed the principles of operation of the flow damper and successfully established the ACC flow characteristics. Specifically, the testing confirmed that:

1. No vortex was formed during large flow and a stable vortex was formed during low flow in the vortex chamber
2. Sharp flow rate switching occurred without gas entrainment.
3. The flow characteristics of the flow damper were organized by dimensionless numbers and were independent with scaling.

Empirical flow rate coefficients have been developed from the test results and will be used in an integrated thermal hydraulic model of the US-APWR Reactor Coolant and ECCS systems to assure the US-APWR meets or exceeds all US safety standards.

The ACC design is expected to improve the safety of pressurized water reactors by the innovative application of the flow damper to assure the early stage of LOCA injection flow is satisfied by an inherently reliable passive system. This innovation reduces the necessity of relying on maintenance sensitive components such as low head safety injection pumps for assuring LOCA injection flow, provides additional time for actuation of backup emergency power for loss of power coincident with a large break LOCA, and reduces the net maintenance and testing burden by the elimination of low head safety injection pumps from the LOCA mitigation strategy.